THE USE OF METAL FILMS IN STUDYING PARTICULATE SULPHURIC ACID IN THE ATMOSPHERE.

THESIS

SUBMITTED FOR THE DEGREE OF MASTER OF PHILOSOPHY

BY

AZARMIDOKHT HAZRATI

Department of Chemical Engineering and Chemical Technology,
Imperial College of Science and Technology,
London S.W.7.

SUMMARY

Droplets of sulphuric acid usually less than 10^{-3} mm. in diameter are a common and harmful form of atmospheric pollution. They represent as much as 90% of the total acid content in the atmosphere of some cities. The size of these droplets is such that they may remain suspended for a long time in air. In order to detect sulphuric acid droplets and to measure their size distribution and concentration, some investigators have used thin metal films instead of gelatinous on films containing indicators. These investigators studied the spots formed by reaction on the films, and tried to relate the size of the spots with the size of the original drops.

This work is an attempt to measure the acid content of a drop by measuring the reduction in film thickness caused by chemical reaction between an acid drop and a metal film. By taking electron and optical micrographs and measuring the density of spots on negatives with a densitometer, one can estimate the intensity differences between background and spot which can be converted to thickness differences quite accurately.

This determines the weight of metal removed, and hence the equivalent weight of acid. Knowing the atmospheric relative humidity, the size distribution of acid droplets which are deposited on metal film can be estimated from these measurements.

The technique is sensitive, since 10^{-15} g of acid can be detected under the optical microscope, and much less under electron microscope.

ACKNOWLEDGEMENTS

I would like to express my thanks to Dr. M.J.G. Wilson for his guidance, interest and help during the course of this investigation. Also I am grateful to Dr. Kerr for his kindly permission to use the microdensitometer; to Mr. Tyley for his help in construction of a home-made densitometer; to Dr. Presland and all members in his group for their useful discussion and help in using the electron microscope and evaporation unit.

Symbols used in Chapters (1 - 4)

Section (3.1.1)

v = particle terminal velocity

p = particle density

g = gravity acceleration

d = particle diameter

η = air viscosity

P = pressure of air or media

Section (3.1.2)

$\frac{ds}{dt}$ = rate of evaporation

D = diffusion coefficient of evaporating molecules.

m_2 = weight of evaporating molecule.

ρ = drop density

c_o = concentration on surface of drop

c_∞ = vapour concentration on far distance from drop

γ = drop surface tension

r_o = drop radius at time zero

r = drop radius at time θ

Re = Reynolds number

Section (3.1.3)

n = particle number concentration at time t

n_o = particle number concentration at time zero

l = mean free path of air

R = gas constant

T_s = absolute temperature

Section (3.5.6)

a = projected area of particles

D_x = number concentration

h = depth of suspension where light beam is passed.

t = thickness of suspension where light beam is passed.

λ = wavelength of light

n = refractive index of metal films

I = transmitted light intensity

I_o = incident light intensity

ρt = mass thickness of metal film

$\gamma S/A$ = surface tension of solid and air

$\gamma S/L$ = surface tension of solid liquid

$\gamma L/A$ = surface tension of solid liquid air

θ = contact angle

S = spreading coefficient

D^o = density

E = exposure (Intensity x time)

D = acid drop diameter

d = spot diameter

h = metal thickness

t_2 = depth of pit

$\frac{dr}{dt}$ = rate of evaporation

$P, P\phi,$ = vapour pressure of evaporating substance in atmosphere and on the drop respectively.

CHAPTER 1.

"INTRODUCTION"

(1-1). Air Pollution in General:

Anything which is emitted into the air and interferes with the amenities of life may be called pollution. The commonest and also one of the most harmful pollutants are gases and particles which are emitted from domestic and industrial chimneys and in other words can be called the combustion products.

Those particles which are in range of(0.5 - 5)μ (1 μ = 1 micron = 10^{-4} cm) diameter which is the respiration range, mostly remain in suspension in air and are the most harmful ones. As Whytlaw-Gray and Patterson suggest, the number of particles observed in the open air is merely the result of a dynamic equilibrium between the rate of generation of particles and the rate of removal by coagulation, sedimentation and turbulent diffusion.

There are two main types of pollutants as particulate matter. 1) Smoke: The size of smoke particles varies from submicroscopic to large aggregates. Waller (1963) and his co-workers reported that in the centre of London where most heating is by large installation burning oil, coal and coke smokelessly, the aggregates were usually smaller than where heating was still with untreated coal. 2) Chemical liquid droplets: Air pollution from chemical industry has provided many cases where the emission of particulate has created health hazards. An example is sulphuric acid mist. Sulphuric acid is one of the pollutants which is partly emitted from sources in chemical industry and partly made by oxidation of sulphur dioxide to SO_3 which is dissolved in water droplets

existing in air. It is not necessary for the relative humidity to be 100% for this reaction to occur. These small acid droplets which are formed remain as part of suspended matter in urban air. The presence of acid droplets in London air has been reported for many years. Commins (1963) reported that the major part (90%) of the acidity of the droplets can be attributed to sulphuric acid. Special attention has been made to fog in which the rate of formation of sulphuric acid from sulphur dioxide may be increased.

Sulphuric acid was one of the pollutants considered as a possible cause of the increased morbidity and mortality noted during the London fog of December 1952. (Ministry of Health 1954). It can be also regarded as a very powerful corrosive material in atmospheric pollution.

CHAPTER 2.

PREVIOUS WORK

(2.1) Gelatinous film method: Most of the work is done by sampling the air by cascade impactor, either 5-stage or Anderson 7-stage. Except for a specially-designed cascade impactor used by Junge, the impactors did not have high efficiency in sampling droplets smaller than 0.5 μ diameter. Junge reported acid droplets to have effective drop size $<0.2\mu$ sampled by his special type of impactor. ((By E.D.S., it means size on which 50% of droplets collected, can be derived from size dis-)). The highest reported concentrations were under relative humidity (R.H.) between 80 - 95%. Nearly all investigators used this method measuring acid concentration by chemical micro-analysis and estimated the size by using calibrated instruments for sampling. They first calibrated their sampling instrument with particles of known size and then used it for sampling acid droplets. For detecting these drops Waller (1963) used coated slides with a gelatinous film containing thymol blue as indicator for acid droplets. He mentioned that this method is not quantitatively valid in high humidities. Lodge, Ferguson and Havlik (1960) reported a rather more accurate method for the analysis of micron size acid droplets using a special solution containing bromophenol blue as indicator. As a result of hundreds of experiments, they reported a formula:-

$$D_h = 2.5\ D_d$$

where: D_h = diameter of reaction spots,

D_d = diameter of pure sulphuric acid droplet.

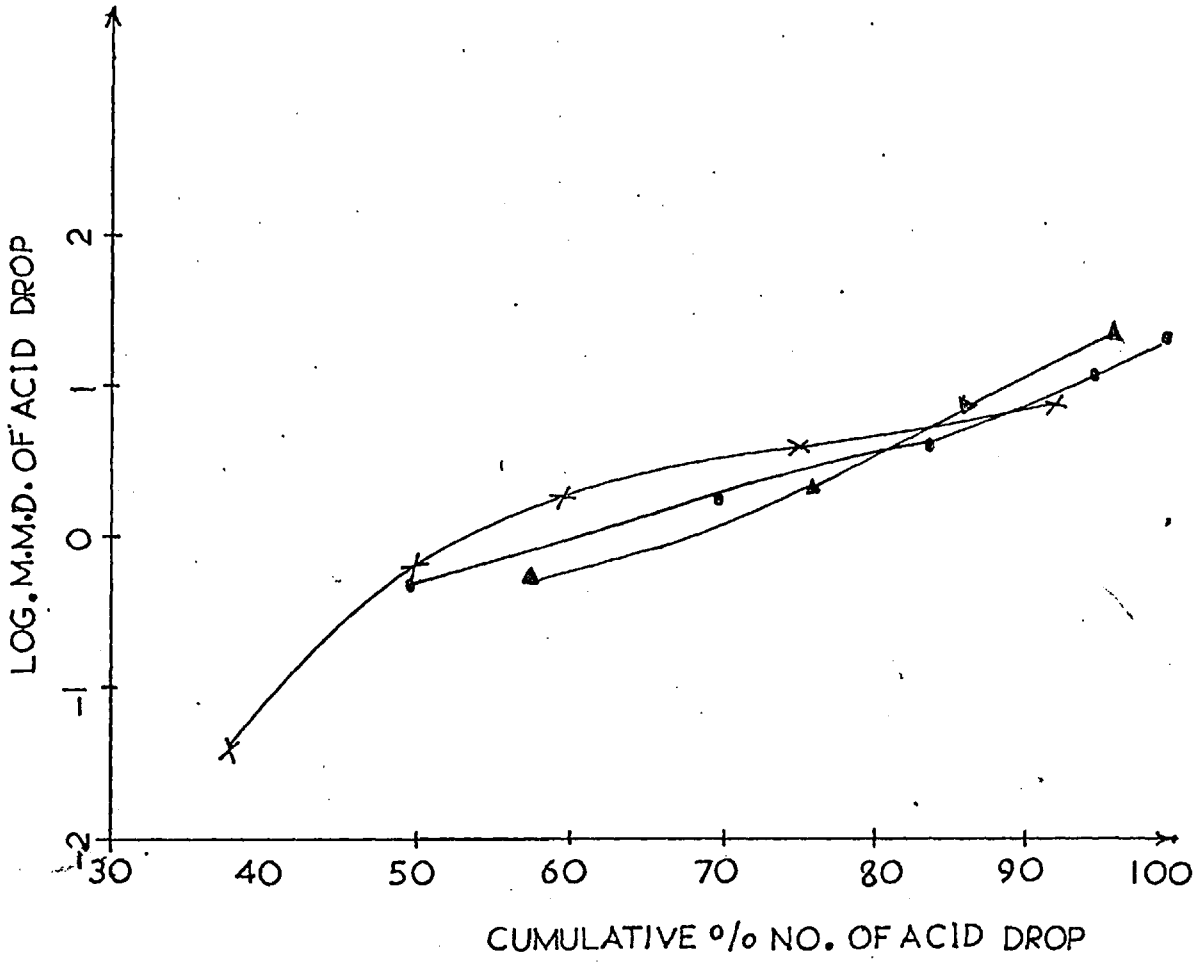


Figure (2.1) Log. Mass . Median Diameter of Atmospheric Acid Drop vs. Size of Droplets. –x–x– Reported by Wallter, •—•—• reported by Morton Corn and ▲—▲—▲— reported by Roseler.

But they also mentioned that this formula is only valid when relative humidity is less than 90%. In the following table, and plotted charts, you can see the results of some of these investigations.

As can be seen from Table (2.1), all these papers give the mass median diameter or effective drop size of sulphuric acid droplets as about 0.5 μ and the concentration varies from 7 μg per $\mu g/m^3$ in summer to 38 $\mu g/m^3$ in winter.

An extreme condition is reported by Cummins where the sulphuric acid concentration was measured to be 600 $\mu g/m^3$ in a period of fog in London (December 1962).

Because a sufficient amount of acid for chemical micro-analysis can be sampled only in a period of fog when R.H. is high, the above mentioned method is not reliable for sizing as reaction spots are affected by high humidity. Also, submicron droplets which are a major proportion of the sulphuric acid drops, cannot be traced with this method.

(2.2) Metal film technique: J.P. Lodge and B.R. Havlik (1960) used vacuum evaporated metal films as indicators of atmospheric pollution. They studied atmospheric corrosiveness by studying total increase in light transmission through a sheet of metal a few hundredths of micron which was exposed to outdoor pollution for a very long period of time (one or two weeks). They studied different metals like copper, iron, zinc, silver and lead and mentioned that different thicknesses do not make any difference in light transmission. They also measured electrical resistance of exposed metal films. They removed dusts from surfaces of metal using moist cotton wool. They gave mean of measurement of corrosive materials in three locations in a period of ten months in 1958. In 1961, Hayashi, Koshi and Sakabe developed the above method for detecting acid droplets in which gelatinous film containing indicator was replaced by thin metal film. They mentioned that reaction spots are not affected by change of humidity in the air. They determined the drop size of sulphuric acid mist by using very thin metal films which were deposited on glass slide by vacuum evaporation. In their experimental work, they usually used iron and copper evaporated films. They exposed these metal films to atomized acid mist, either 2N or pure. Their experiment led to a relation between size of the holes formed and the initial size of the droplets:

$$D = ad^{2/3} - b$$

where D = droplet diameter

d = reaction spot diameter

a, b are constants.

From this formula disregarding contstants, it is seen that they related volume of droplet to volume of cylindrical hole

or pit in metal. They gave values of the constants, a, b for iron and copper when exposed to 2N and to pure sulphuric acid droplets. They referred to the reaction results as holes. I calculated the depth of the pits by applying their general formula to the conditions of each of their experiments:

% of acid drop	Metal	Depth of pit or thickness of metal A^{o}	D=drop diameter μ	d= μ reaction spot diameter	d/D
10%	Copper	29.8 A^{o}	4	10.5	2.6
100%	Copper	150.0	4	20.9	5.2
10%	Iron	12.9	4	17	4.2
100%	Iron	155.0	4	19	4.8

Table (2.2) Calculated Depth of Pit or Thickness of Metal Film from Experimental Formula Derived by Hayashi et al.

Note: So either their metal films were very thin and these spots were indeed holes right through the films or the films were thicker and the holes were merely pits having the depth calculated above. The smallest droplets which were studied by Hayashi et al were few micron in diameter. S.W. Horstman and J.W. Wagman (1966) did another set of experiments on sizing acid droplets by using metal films. They used

sulphuric acid mist which was made either with a nebulizer or in a LaMer generator by condensation. The metal films were exposed to the mist and then studied by optical and electron microscopy. They only counted reaction spots and by using thin metal films in deposition area of a calibrated Goetz aerosol spectrometer, they computed least-square curves for size of collected materials which then were converted to size distribution curves. They mentioned optimum thickness for iron film to be (0.4 - 0.6) micron. These thicknesses seem too high as will be discussed later. They estimated the diameter of the reaction spots on iron film to be roughly 1.5 times the diameter of the incident acid droplets. They reported M.M.D. of sulphuric acid droplets for $\rho = 1$ to be 0.35 micron.

Homma and Sakable (1967) used very thin metal films to study the effect of high humidity on the reaction between films of various metals and silica gel particles which had been exposed to an aqueous solution of sulphuric acid and sulphur dioxide. As the result of their experiment, they reported that thin metal films were affected by silica gel particles containing acid when they were exposed to water vapour. In lower humidities, they could see no effect of reaction between particles and metal films. They used silver and copper films with thicknesses assumed to be (50 - 100)A^{o} ($1A^{o} = 10^{-8}$) cm. They reported no quantitative results. As far as I could find in published papers, these are a few works whibh are done in using metal film technique to detect sulphuric acid droplets.

CHAPTER 3.

Notes about Problems Associated with the Subject

(3.1) Some properties of mist relevant to this work:

mists consist of droplets usually formed by the condensation of the vapour upon the nuclei or sometimes by atomization of liquids. In other words, mist is essentially manifestation of disperse systems in which liquid substance is dispersed in a gaseous medium, the atmosphere. The sizes of the droplets are expressed as their diameters. Natural mists usually carry substances in solution or particles in suspension.

(3.1.1) Rate of fall of particles: when a particle in the Stoke's region (i.e. when mean free path of air $<$ particle size $<$ size at which any effect arises from gas displacement) settles in still air, it soon reaches a constant terminal velocity. In this case, the aerodynamic drag on the particle is equal to its' weight.

Terminal velocity is given by:

$$v = \frac{\rho g d^2}{18\eta}$$

Density of gaseous media which is usually small assumed to be negligible in comparison with particle density.

For particles with diameter up to 29μ when P = 1 and are falling in air, the deviation from Stokes' law is 1%. Stoke's law should be corrected with Cunningham correction factor when the particles are small to be comparable with the mean free path of air molecules ($\simeq 0.1\mu$).

$$v = \frac{\rho g d^2}{18\eta} \quad (1 + 2A\lambda/d)$$

where λ is mean free path of air.

Davies C.N. (1947) derived an expression for this factor for particles falling in air in 20 °C (normal temperature):

$$\text{Cunn. Corr. Fac.} = \frac{1 + 2 \times 10^{-4}}{Pd} (6.32 + 2.01 \exp(-1095\, Pd))$$

e.g. Correction factor is 1.164 for = 0.5 μ

and 11.554 for = 0.01 μ

(3.1.2) Evaporation and growth of droplets:

Experimental work on the rate of fall of freely falling droplets proves that for a substance with vapour pressure as low as 10^{-4} mm. mercury, their life-time is not still more than a few minutes even at normal atmospheric condition. Langmuir (1918) and Maxwell (1890) gave the formula below for the rate of evaporation of droplets:

$$-\frac{ds}{dt} = \frac{8\pi D m_2 C_o}{\rho}$$

$$\frac{dm}{dt} = 4\pi D m_2 C_o r$$

Langmuir's formula can be written as:

$$r_o^2 - r^2 = \frac{2D}{\rho} (C_o - C_\infty)\tau$$

which gives rate of evaporation in interval of time τ. The above formula cannot be applied for very small particles (much smaller than 1 μ diameter) and also is not applicable for very low pressures.

If the rate of fall in temperature on drop surface is significant D must be replaced by $\sqrt{D_o D_\infty}$, where, D_o is the value of D at the temperature of surface of droplet. Very small droplets can be regarded for calculating the rate of evaporation and growth, as stationary droplets. If droplets

are ventilated by air with different velocities:

$$\frac{dm}{dt} = 4\pi rd\left[(C_o - C)\,(1 + a(Re)^{\frac{1}{2}})\right]$$

or $$\frac{dm}{dt} = \left(\frac{dm}{dt}\right)_o f$$

$\left(\frac{dm}{dt}\right)_o$ is the rate of evaporation of droplet in still air and f is called the ventilation factor.

It is very important to know that presence of impurities may retard the evaporation and even bring it to a standstill.

(3.1.3) Factors which alter size distribution of droplets in mist: In high concentration particles collide when they come into contact. Whytlaw-Gray (1932) showed that coagulation of many particles follows this formula:

$$1/n - 1/n_o = Kt$$

K is coagulation constant and t represents time.

or $$\frac{dn}{dt} = -Kn^2$$

although K varies from one aerosol to another, the coagulation process does not depend on the nature of the aerosol.

e.g. In stearic acid mist $K = 0.51 \times 10^{-9}\ \frac{cm^3}{sec}$

$$n_o = 10^{11}\ , t = 0.02 \rightarrow n = \frac{no}{2}$$

These are the factors which increase the rate of coagulation:

1.- Coagulation rate increases rapidly as average particle size falls.

2.- Polydispersity: It is proved by Smoluchovsky's formula

and theory which is illustrated by Fuchs (1934) that the rate of coagulation:

$$\frac{dn}{dt} = \frac{RT_s}{6\eta N} \frac{(r_1 + r_2)^2}{r_1 r_2} (1 + \frac{Al}{r})n^2$$

$S = \frac{1}{2}(S_1 + S_2)$ and S_1 and S_2 are radii of sphere influence of particles. Thus for $r_1 = r_2$ the above equation is minimum.

3.-For mist containing coarse droplets, the bigger ones collide with others when they settle. This phenomenon which is called "Orthokinetic" coagulation is negligible for mist of fine particles.

4.-Temperature, pressure and viscosity of gaseous media affect the rate of coagulation.

$$K = 4RT(1 + Al/r)/3\eta$$

5.-Van der Waals force of attraction between particles increases the rate of coagulation with a factor γ which is independent of size.

$$K = \gamma \frac{4RT}{3\eta} (1 + Al/r)$$

6.-Stirring increases rate of coagulation quite markedly.

(3.2) Preparation of mist:

(3.2.1) By condensation method: This method was achieved by La Mer and Sinclair (1949). The generator which was devised by them was and still is widely used in investigations on aerosols. The basis of this generator is vaporisation of liquid and condensation of vapour on foreign nuclei in a double-walled chimney (except for sulphuric acid where foreign nuclei are not needed because it is a self-nucleation substance). 99% sulphuric acid has proved to be suitable for homogeneous mist generation in this generator.

The acid droplets made in this device if necessary can be increased in radius nearly 8 times by exposing them to aqueous solution of acid with higher water content. 10^6 is the maximum number concentration for stable mist.

Rapaport and Weinstoke devised a much simpler instrument. The degree of monodispersity is not as high as in the La Mer generator and the size of drops is in the range (0.508 - 0.540)μ, but it takes only a few minutes to reach steady-state condition.

Standard deviation σ is reported to be (3-8.5)% and concentration is $(5 \times 10^4 - 10^8)/cm^3$. The initial mist which is needed is made in a nebulizer giving 3.7 lit/min min heterogeneous aerosol.

A Rapaport type generator was used by the Scientific Department, Ministry of Defence, Tel Aviv, Israel (1955). In this generator a Dautrebande nebulizer is used and provides a sharp upper limit for aerosols equal to 1.2 μ Standard deviation is (20 %- 30%) for size distribution of droplets made.

* Other methods to generate monodisperse condensation aerosols are:

1.) Mixer type condensation aerosol devised by Kogan (1960). I., and S. Burnashera, (1960).

2.) By chemical process method: in range of size (0.15 - 0.4) with relative standard deviation α ($\alpha = \frac{\sigma}{\bar{x}}$) equal to 0.10, devised by G. Goyer and G. Handler, (1955).

(3.3.2) By dispersion method: The theory is fully discussed by N.A. Fuchs and A.G. Sutugin in Aerosol Science.

This method includes several submethods:

a) Atomization of liquid using capillary tips;

$$G = \frac{4}{3}\pi r^3 \rho g = H = 2\pi R \gamma K$$

H is capillary force and G is gravitational force. K is a constant of order 1.

By using this method, F. Buckholz and M. McPhail (1960) made droplets with radius in range of (22 - 220)μ and relative standard deviation α in range of (0.11 - 0.05). These instruments devised and used in this method usually have very low output and rather high dispersity.

b) Vibrating capillary atomizer: D.J. Ryley and M.R. Wood (1963) using instrument based upon this method reported size of droplets in range of (300 - 1350)μ for vibrating frequency≈3000 c/s.

B.J. Mason, O.W. Jayaratne and J.D. Woods (1963) reported from an instrument 4 cm., 30 gauge recorder and needle driven at point 3 cm. from its tip resonate at about (300 - 1000) ± 10 c/s a size range of drops of (500 - 15)μ.

c) Disc atomizer: if surface of disc is well wetted and liquid is fed accurately to the centre of the disc, then much smaller uniform droplets may be formed. In an instrument designed by W. Prewette and V. Walton (1958) drops were made with size down to 8μ for angular velocity ω = 1500 r.p.s.

Disadvantage of disc atomizers is that, the droplets spread out in all directions.

(3.4) Sampling of mist.

(3.4.1) Gravity settling: this is a rather easy but slow method and technique has many disadvantages. Because the bigger particle settles much faster, the deposited smaple has not exactly the same size distribution as the pollutant itself.

(3.4.2) Filtration: The commenest devices for aerosol sampling are filters. They make a wide range of analysis possible and improved ones are quite capable of sampling particles down to millimicron size.

Chemically treated filters are used to detect special type materials. When purpose of study is optically measurement of size of the particles, membrane filters with regular pores in range of (10^{-3} - 10)μ are widely used, because they collect materials on the surface of the filter.

(3.4.3) Precipitators: Particles can be precipitated from gas by thermal or electrical gradients. Thermal precipitators are not widely used for practical aerosol sampling due to difficulties in operating, limitations on instrument and effect of rather high temperature on size distribution of droplets of volatile substances. Electrical precipitator is used to sample sufficient quantity of aerosol to allow macrc-chemical analysis.

(3.4.4) Impactors: When a jet of air is directed against a flat plate, particles will resist this rapid change in direction and will tend to impinge against the plate. By increasing gas velocity, the probability of smaller particles hitting the plates increases. Well designed instruments based on this technique are called Cascade-Impactors. These are not quite efficient for the collection of small particles (submicron), because the acceleration in jets should be quite

high to remove submicron particles. Impactors are relatively simple and have ability to classify particles in range of size. They are widely used in the field of air pollution sampling.

(3.5) Measurement of mist size and concentration:

(3.5.1) Optical method: This method is usually used for concentration measurement and is applied to samples taken on filter papers. By using a reflectometer which is calibrated for reflectance against weight of black materials, concentration of pariculate matter can be estimated. J. Coulson and M. Ellison, used a FG/A glass filter paper to avoid effect of humidity for providing a calibration method. They reported that relationship between logarithm of reflectance and mass of material is not linear.

(3.5.2) Size measurement by magnesium oxide method: An optical microscope is used to measure trace of droplets on magnesium oxide layer. It is experimentally proved that spots have constant relation to initial drop diameter. Care should be taken to ensure that thickness of layer is a bit bigger than diameter of biggest droplet sampled. This is only convenient for detecting droplets bigger than 5 diameter.

(3.5.3) Absolute method: by this term is meant a method in which the drops are mounted for examination in their original spherical form so that no correction for apparent size is necessary. They are mounted in a matrix with a similar density, high viscosity and rather different refractive index in which they are insoluble. This method is widely used for water drop measurement e.g. by Fuchs and Petrjanoff and K.R. May, etc. A thin uniform layer of matrix is spread with gentle heat on a slide and a cover slip containing a drop

of matrix is heated so that the matrix is melted and then is pressed gently on the slide after sampling. If temperature of heated cover slip is correct, the molten mixture spreads at once over the sample totally preventing movement of droplets which are drawn up into their original spherical form.

(3.5.4) Light scattering method: This method can be used for measurement of size of monodisperse particles which have sizes comparable with wavelength of light transmitted or the same order as wavelength of light. Since in this range of size Rayleigh-Gauss equation gives angular dependence of intensity of scattered light on average size of droplets. The particles should have known refractive index and usually scattered light is measured perpendicular to incident light ($\theta = 90^0$).

(3.5.5) Light extinction method: This phenomenon is due to absorption of light by particles rather than scattering. This means total removal of flux from the beam traversing the particulate suspension.

$$I = I_o \exp(-na\,Et)$$

where I and I_o are intensity of transmitted and incident light, n is number concentration, E is extinction coefficient and t is thickness of suspension. If mist is polydisperse naE must be integrate over the particle size distribution. Or for constant E, $\underline{a}$ can be regarded as mean projected area of particles.

(3.5.6) Photosedimentation technique: This technique is a combination of photoelectric measurement and gravitational settling of particles. A narrow beam of light is projected horizontally at a depth h through a homogeneous suspension

on to a photocell. When a set of large particles fall from the measurement zone, the attenuation of the light beam will fall. So the concentration of particles in beam now must be the concentration of particles smaller than D_x which is given by Stokes' equation:

$$D_x = \frac{18\,\eta}{(\rho_s - \rho_f)g} \cdot \frac{h}{t}$$

The relation between attenuation of light and concentration of particles can be derived from Bouguer Law as mentioned in section (3.5.5). H,E, Rose (1952) and T. Allen (1962) used this technique for size and concentration of particles comparable with wavelength of light used.

(3.5.7) Optical and electron microscopy:

1.-Optical microscopy: to determine the size distribution of a mist, one of the commercial methods is to study samples taken on slides under an optical microscope. The main part in this set of measurements is that the resolving power or in other words, the useful magnification of system should be considered, otherwise the results will be quite misleading.

2.-Electron Microscopy: The only specimens that can be studied by this device are those which do not contain particles of volatile substances or any other materials which are liable to be damaged when exposed to electron beam. Otherwise it is the best device for very fine particles measurement because it's useful magnification can exceed 10^5x.

(3.6) Properties of light: the fundamental theory of functions named in this section are all well expressed and explained in optical text books (names are given in reference section). A summarised review can be seen in the next sections about the parts which are related to the optic of metal films.

(3.7) Metal films;

(3.7.1) Preparation of thin metallic films: the method available for the preparation of thin films by building up are as follows:

1.- Sputtering: The ejection of atoms from the surface of material by bombardment with energetic particles is called "sputtering". It is usually due to positive ion bombardment and is called cathodic sputtering. The sputtered atoms can be condensed on a substrate to form a thin film. A new and complete technique is used in experiment by P.K. Rol, D. Onderdelinden and J. Kistemaker (1965) and a complete comprehensive report is given by Holland.

2.- Electrodeposition: The experimental arrangement requires a suitable electrolyte through which current is passed between two electrodes. The deposition rate is proportional to the electrolysis time and the current density, and varies from (1A^{o} to few μ) per second. The technique is used by K.R. Lowless to provide thin metal films.

3.- Chemical vapour deposition: when a volatile compound of substance to be deposited is vaporized, the vapour is thermally decomposed with other gases, vapour or liquids at the substrate to yield non-volatile reaction products which deposit atom by atom on substrate. This is a widely used technique for producing deposits of pure metals. Technique is used and developed by P.J. Jorgenson (1962).

4.- Vacuum evaporation: The commercially available vacuum evaporation units are well suited for the purpose of vacuum evaporated thin films. The thickness of the thin film formed can be estimated from the amount (mass or length) of metal evaporated for materials which evaporate without alloy formation:

$$t = \frac{m}{4\pi r_1^2 \rho}$$

where m is the mass of material with density ρ evaporated. r_1 represents distance between stage and substrate. Holland (1956) describes relations for other arrangements.

Below is the list of a few methods which are used for thickness measurement of thin films:

a) Rate monitors: gives a meter reading either of film thickness or rate of deposition (Beckerman and Thun (1962)).

b) Weighing: for thicker films than 300 A^o in which a microbalance is used which can be mounted in vacuum chamber (Clegg and Crook (1965)).

c) Micro chemistry: this method has accuracy $\pm$ 20 A^o for films 800 A^o thick (Heavans (1959)).

d) Radio-active tracer technique: only applicable accurately to materials for which a suitable isotope is availabe, (Preuss (1953) applied method for gold).

e) Fizeau fringes: this is fully discussed by Heavens (1959)).

(3.7.2) Properties of metallic thin films:

1.- Physical property: thin metallic films formed by vacuum evaporation have usually a polycrystalline structure.

The crystalline size of metals increases with increasing surface mobility of adatoms during deposition on substrate. The crystallite size of films decreases with decreasing deposition temperature. At very low temperature of substrate adatom mobility is so low that an amorphous deposit may form. Whether this deposit consists of tiny crystallite or not is immaterial and as long as there is no long range order, its property can be regarded as amorphous. M.J. Fuks, L.S. Palatnik, and B.T. Boiko (1966) studied cool stage deposition for aluminium (60 - 200 A^{o}).

Surface roughness: under suitable deposition conditions, atomically smooth surfaces can be obtained usually for films with fine-grained and amorphous structure. The roughness factor which is the ratio of real to geometric surface area tends to unity for films deposited at low substrate temperatures.

2) Optical properties: Optical property of an dielectric can be explained solely in term of n, the refractive index at any wavelength of light. But for a metal layer another constant must be specified which measures the strength of absorption of light as it enters the metal. Light absorption is very strong in metals so that intensity of light falls practically to zero in a small fraction of wavelength. The most important factor in light absorption by metals is the absorption index k which is defined in terms of the absorption coefficient α and K_o:

$$K = \frac{K_o}{n} \text{ and } K_o = \frac{\alpha\lambda}{4\pi}, \text{ so } \rightarrow K = \frac{\alpha\lambda}{4\pi n}$$

The optical properties of metal films thicker than 100 A^{o} are not very much dependent on their microstructure, but thickness dependence can be still seen in thin metal films.

Note: From equation of path difference for normal incident light, it can be derived that:

$$2 n_1 d = 5\lambda$$

$$\therefore d = \frac{5/2\lambda}{n_1}$$

e.g. $n_1 = 1.5$ for $\lambda \approx 0.6$

$$\therefore d = 1\,\mu$$

It means that for materials with nearly this refractive index deposited on glass supports, films with thicknesses up to 1 μ can be regarded as thin films.

3) Light absorption by metal film:

The intensity of light transmits through an absorbent layer usually is attenuated in a exponential form of the type e^{-KT} where K is absorption coefficient. The wave equation of light can be modified to take account of absorption by multiplying the amplitude by the factor $e^{-\alpha x/2}$ or $e^{\frac{-4\pi nk}{2\lambda}}$ since the amplitude varies with (intensity)$^{\frac{1}{2}}$.

Overall, regarding a thin metallic film as an amorphous layer, Lambert's law can be simply applied ($I = I_{oe}^{-\alpha t}$) to explain absorption through these films.

So it can be said that this decrease in light intensity is directly related to the thickness of metal film. By applying Lambert's law to two layers of different thickness we can derive the equation:

$$I_2 = I_1 e^{-4\pi nk(t_2 - t_1)/\lambda}$$

(I_2, t_2) and ($I_1 t_1$) represent intensity and thickness of two

layers respectively. t and λ must be expressed with the same unit. With the above expression, it can be seen that nk can be measured from measurement of transmitted intensities through two different known thicknesses of a substance. In this way, the error due to reflection from the surface of substance also can be avoided.

4) Electron absorption: It is well known that the following relation exists between the object mass thickness ρt and decrease of electron beam intensity passing thrpugh specimen and background immediately adjacent to the specimen respectively:

$$I_s = I_B e^{-S_t \cdot \rho t}$$

I_s and I_B are intensities of electron beam transmitted through specimen and background. S_t is called "total mass scattering cross section of electron."

If ρt is known by measuring the contrast of an object in the image plane (contrast K = log IB/Is), one can estimate the value of S_t of specimen under the operating condition of electron microscope as:

$$S_t = K/\rho t$$

Investigators like Hall, Bahr and Zeitler, experimentally proved that for ln(Io/I) up to 3, the exponential relationship is valid and for ρt within the range of (1 - 100) $\mu g/cm^2$, contrast is directly proportional to the mass thickness of the specimen. The last mentioned proportionality will be discussed again in the next chapter.

(3.8) Contact angle: If a small drop of liquid is placed on a uniform, perfectly flat, solid surface, it will in general not spread completely over the surface, but its edge will make an angle θ with the solid called the contact angle (Figure (3.1).

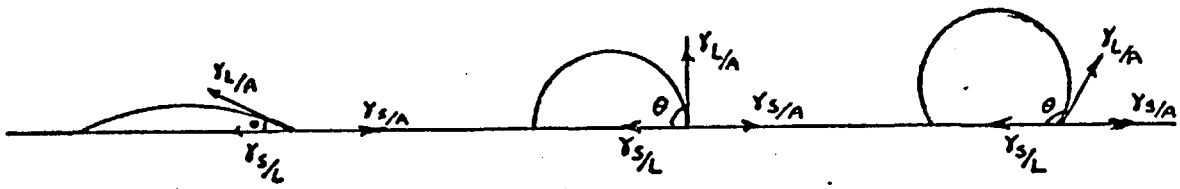


Figure
(3.1) Different type of deposition of drop on solid surface.

If we write horizontally equilibrium tension acting from figure (3.1) we can write

$$\gamma_{S/A} = \gamma_{S/L} + \gamma_{L/A} \cos \theta$$

If we write famous Dupré equation $W_{S/L} = \gamma_{S/A} + \gamma_{L/A} - \gamma_{S/L}$ and combine these two equations together we can derive another equation:

$$W_{S/L} = \gamma_{L/A} (1 + \cos \theta)$$ Young's equation

where $W_{S/L}$ is called work of adhesion.

The contact angle depends on: 1) roughness of the surface - surface roughness increases θ if it is more than 90^0 and decreases θ if it is smaller than 90^0. If we assume roughness coefficient to be v(this factor is described in the section (3.7.2), we can write $\cos \bar{\theta} = v \cos \theta$. $\bar{\theta}$ and θ represent real and/or theoretical geometrical contact angles respectively.

Spreading: By analogy with the spreading coefficient of one liquid on another:

$$S = \gamma_{W/A} - (\gamma_{O/A} + \gamma_{O/W})$$

we may write for the spreading coefficient of a liquid on a solid:

$$S_{S/A} = F_{S/A}^{S} - (\gamma_{L/A} + F_{S/L}^{S})$$

where F^S is surface energy for unit area.

Combining the above formula with:

$$F_{S/A}^{S} = F_{S/L}^{S} + \gamma_{L/A} \cos \theta$$

we can write:

$$S = \gamma_{L/A} (\cos \theta - 1)$$

which is valid for $\theta > o$.

S can be determined by measuring experimentally ($\gamma_{L/A}$ and θ) or ($\gamma_{L/A} \cos \theta$).

These methods are explained in experimental work by: Adam and N.K. Livingston, (1958).

(3.9) Chemical reaction between acid droplets and thin metallic films:

Reaction between sulphuric acid droplets and a thin metallic film does not necessarily follow exactly the same course as reaction between these two substances in bulk. These are some discussions about reaction of mono-layers in surface chemistry and surface science text books, but, no satisfactory information was found on chemical reaction of thin metallic films. So we have to consider in this investigation that this chemical reaction is similar to the original reaction between sulphuric acid and metals. Sulphates which are obtained from reaction between sulphuric acid and metal oxides are mostly water soluble and colourless.

In the presence of an oxide layer on metal, sulphuric acid first penetrates imperfections on the layer surface and then attacks layer-metal interface. Reaction between iron and dilute sulphuric acid usually produces ferrous sulphate.

If ferrous sulphate is heated in the presence of concentrated sulphuric acid, ferric sulphate is formed.

The rate of reaction of sulphuric acid and nickel is very slow. Concentrated sulphuric acid does not

show any severe effect on iron and nickel. This inertness is caused by the formation of a black deposit on the metal surface which protects the metal from further action of acid.

CHAPTER 4

EXPERIMENTAL PROCEDURE.

(4.1) Choice of method for mist preparation:

The condensation method was not chosen because it was not critically important to have monodisperse mist and because a condensation type generator was not available and not worthwhile to make. Generation of mist in this investigation is done by atomization of liquid using an ultrasonic nebulizer.

(4.2) Choice of instrument:

First a system called "microburette" was tried devised by L.G. Abberton. Although it was quite capable of making single drops in range of (20 - 300)μ diameter, it was not used in this investigation because of insufficient cutput droplets produced.

The next instrument used for mist preparation was an ultrasonic nebulizer. This commercial DE VILBISS nebulizer model 900 is designed to provide high density rather homogeneous aerosols for use in respiratory therapy. The ultrasonic power unit in this model develops approximately 1,350,000 cycles per second (1.35 megacycles). Water in a couplant compartment transmits the vibrational energy generated by the transducer into the nebulizer chamber, atomizing the liquid to be administered into minute droplets. The carrier gas used to exhaust the aerosol droplets from the nebulizer chamber can be gas from a compressed gas cylinder. The gas flow rate, either through the chamber or for dilution of mist, is controlled and measured.

To detect the mist made by this nebulizer, it was sampled on a layer of silicone supported on a glass slide when mist was settling under gravity. The slide was then treated as described for absolute method in section (3.5.3) and then studied under optical microscope. From graphs in figure (4.1), it can be seen that the mist, although not accurately monodisperse, does not have a wide range of size. The various curves represent different conditions of operation of the nebulizer.

($\bar{\alpha} = \frac{\bar{x}}{\bar{r}} = 0.24$).

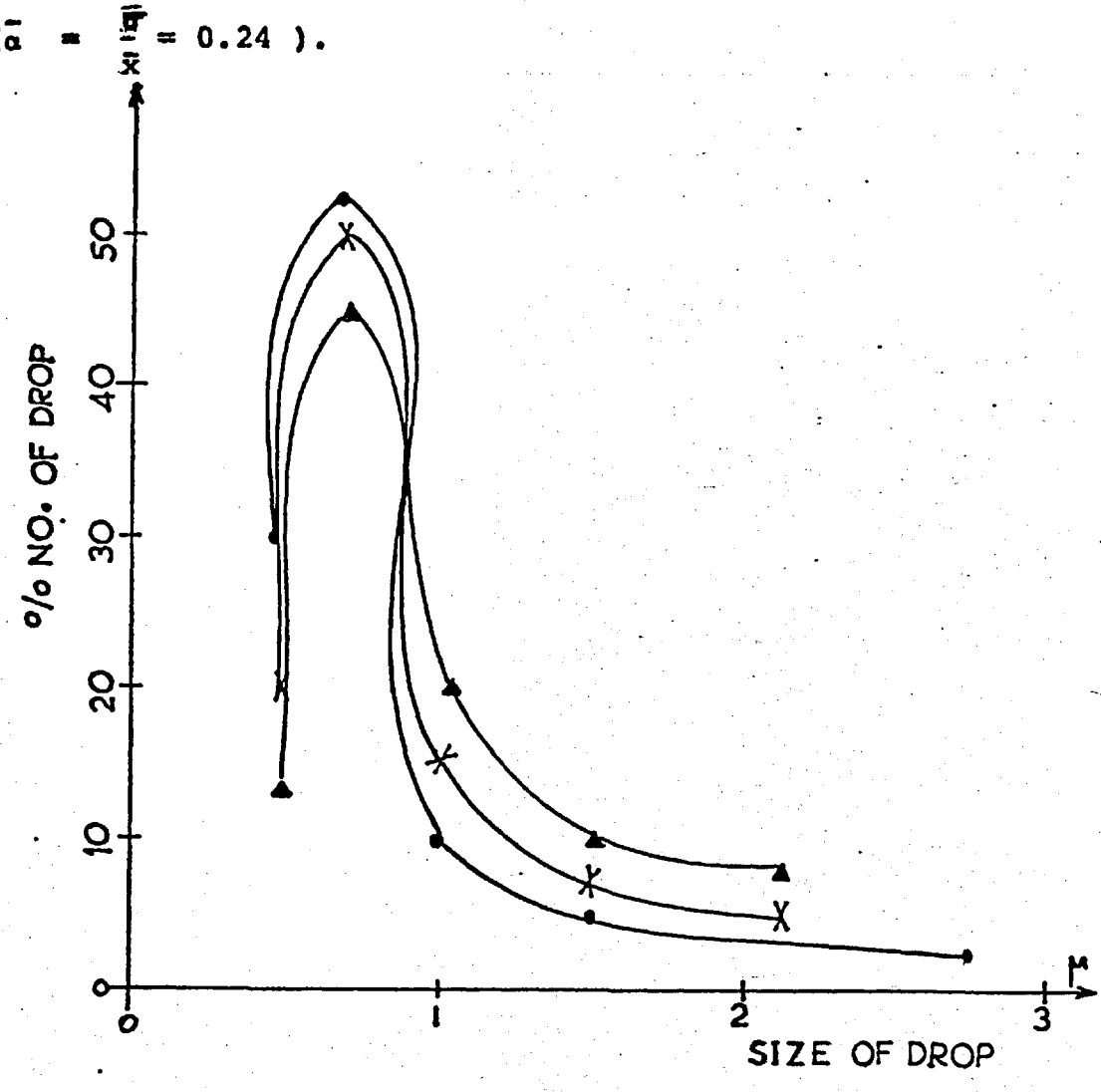


Figure (4.1) Size Distribution of Water Droplets made in Devilbis Nebulizer. Different Curves Represent Different Condition of Operation.

(4.3) Method of sampling:

(4.3.1) Part of sampling was done with a cascade impactor made by Casell Co. This instrument was chosen mainly because it is widely used in air pollution sampling and although it is not very efficient for sampling submicron droplets, it scarcely alters the initial size of particles sampled because it does not cause serious evaporation in the sampling period. Also, it was available when the investigation was started.

This 5-stage cascade impactor which is mainly used for sampling outdoor pollution is designed for qualitative and quantitative sampling in the size range (0.5 - 200)μ (μ = micron = 10^{-4} cm).

The full description of this instrument is available either in its instruction book or in a paper published by K.R. May and C.N. David (in 1956 and 1951 respectively). A diaphragm pump was used to draw 17.5 lit/min flow rate through impactor which is the most suitable flow rate.

The efficiency of each stage sampling is plotted in figure (4.2).

In next page

Figure (4.2.)

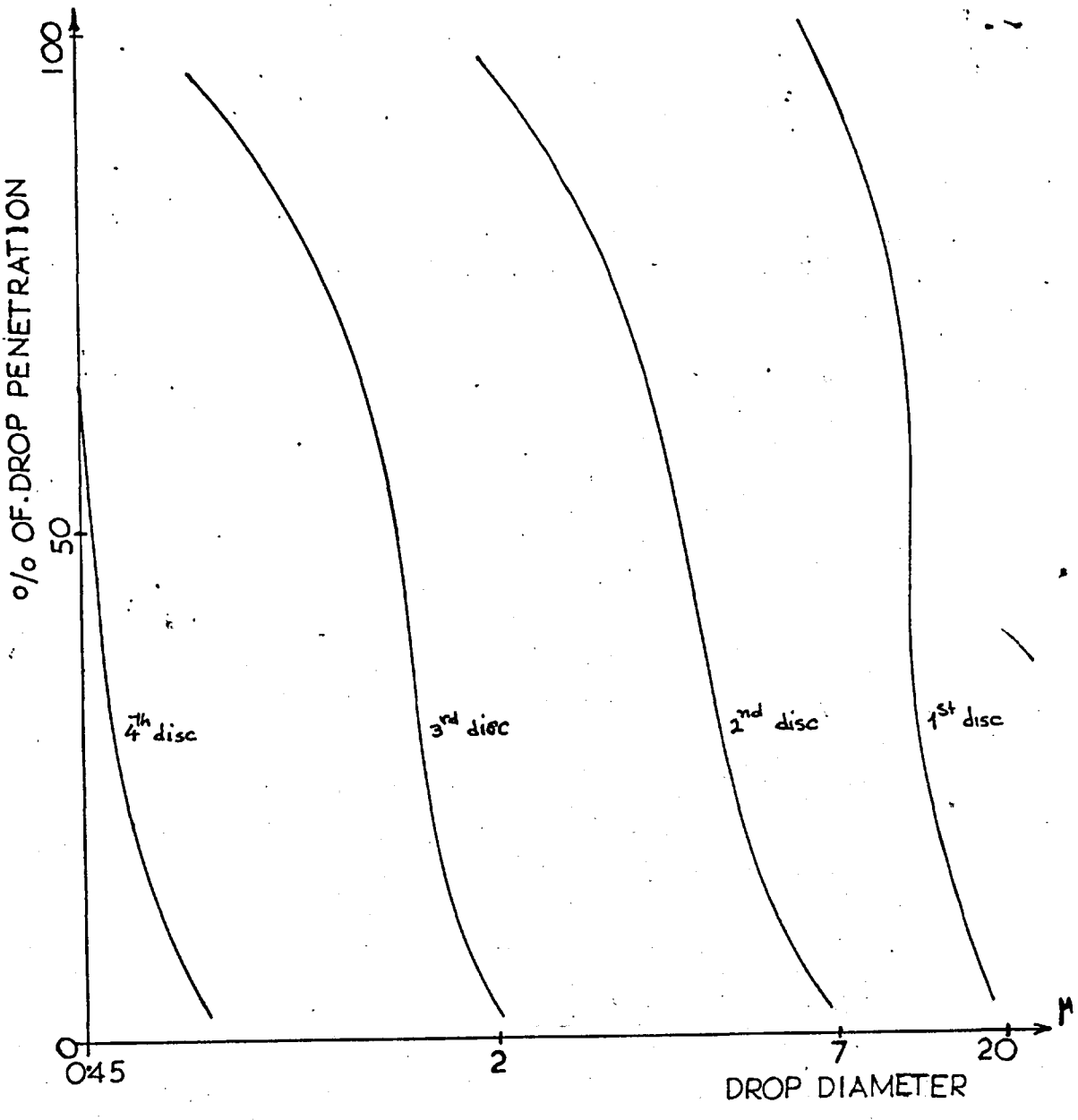


Figure (4.2) Penetration curve for stages of cascade impactor

From Figure (4.2), it can be seen that when four jets are operated in series, the maximum drop size which is found on the first, second and third discs is 20, 7 and 2.5 micron respectively.

In the fifth stage of the cascade impactor a no. 1 Whatman filter paper is inserted to collect smaller particles

(4.3.2) By sedimentation under gravity: the second method which was used, mainly to sample the mist made with the nebulizer, is sampling by settling under gravity. Part of the apparatus was designed to fulfil these two purposes: a) to be completely leak-proof even when sampling slides are changed.

b) to control humidity in the sampling stage accurately with a simple chemical method.

(4.3.3) Description of apparatus used: A glass tube 3" diameter and 40" long is connected at the top to the output of the nebulizer. At the bottom of the tube there is a perspex section containing a shutter and slide sampling stage. The latter is a rod of perspex 1½" diameter in which a flat stage is machined to support a slide. Two sets of 0" rings prevent leakage from this part in any position of the slide-stage. A cylindrical reservoir for humidity-controlling reagents is attached below the slide stage. The slide has a shutter which controls the time that the slide is exposed to settling mist droplets. Excess mist was neutralized by passing through a large vessel containing coneentrated solution of ammonia and was then directed outdoors. The optimum flow rates were found experimentally.

(4.4) Control of relative humidity in sampling device: Although evaporation and growth of acid droplets is not very important in this investigation, since what is measured is the acid content of the droplet, the humidity was controlled approximately in the sampling stage.

A saturated solution of some of a suitable chemical substance at room temperature was placed in the reservoir underneath the sampling stage to provide a suitable humidity for sampling on the metal film surface. Sometimes aerosols were passed through a reservoir partially filled with a master solution of sulphuric acid of the desired normality.

Figure (4.3) is derived from experiments by V.K. La Mer, and I.B. Wilson and shows the dependence of the percentage by weight of acid in the droplet upon the relative humidity.

(4.5) Studying exposed metal films:

(4.5.1) Optical microscope used:

The optical microscope used for size measurement and photomicrography is the "Reichert Diapan" large laboratory microscope. The microscope can provide different magnification by changing objectives adjusted on a rotating nosepiece. It operates with eyepieces 12.5 x and objectives 12.5 x up to 100 x. The 100 x objective is an oil-immersion type. A standard graticule in the eyepiece is used for sizing objects. A stage micrometer is used to determine magnification for each combination of eyepiece and objective. Microphotographs are taken by use of an Exacta camera adaptable to the microscope.

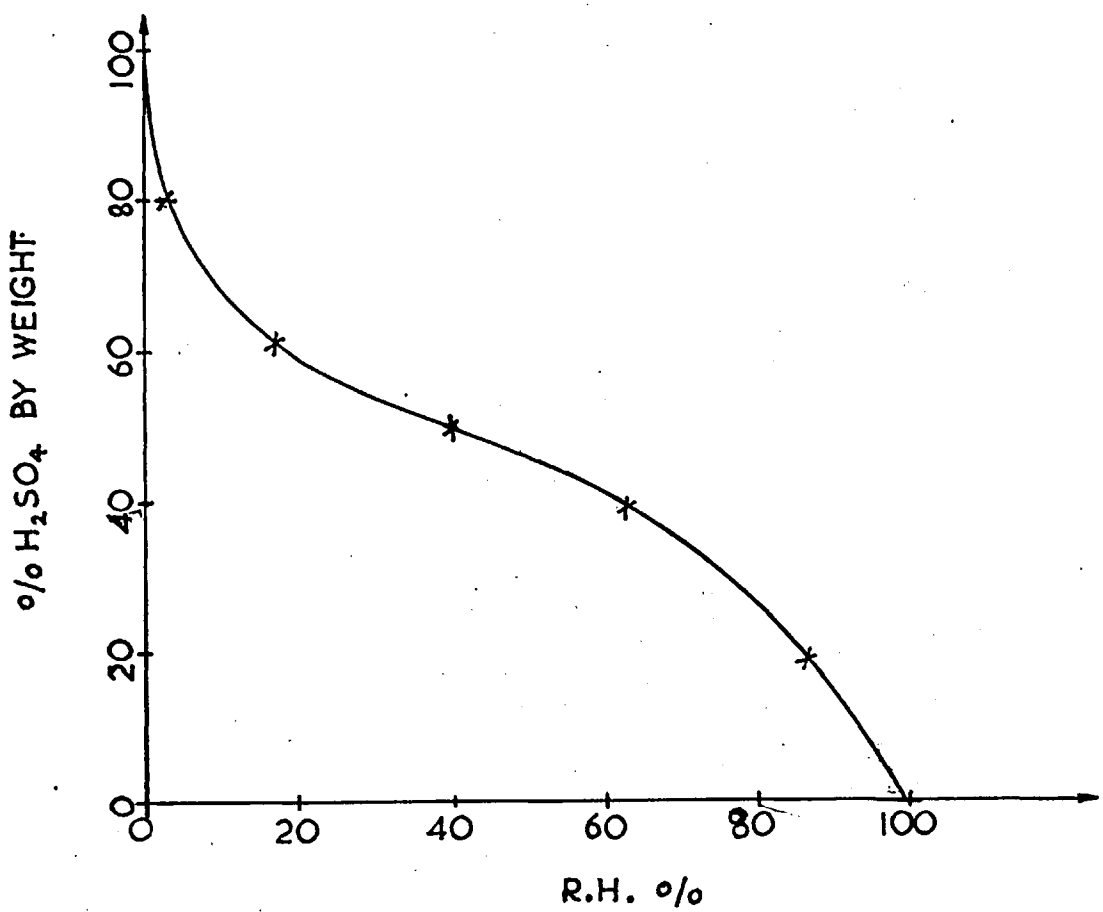


Figure (4.3) Dependence of % by Weight of Acid upon the Relative Humidity.

An interference filter can be inserted in the light transmission system of the microscope to provide monochromatic light with $\lambda = 5890 \pm 10A^{o}$). This filter is used when intensity measurement through reaction spots is necessary. The range of magnification available from this optical microscope using dry objectives is from 150 x up to 780 x. This means that the resolving power of the microscope is from 1.2 μ down to 0.36 μ.

When reaction produced only a very shallow pit, which was difficult to see by transmitted light, a combination of transmitted and incident light was used. It should be mentioned that objects of diameter 0.5 μ were seldom distinguishable from those of 0.7 μ diameter, and they were easily confused.

When the contrast was poor, with thin metal films or suspended acid droplets in a silicone layer, better results could be obtained either by using a green filter or by decreasing the light intensity using neutral filters.

A diffusing filter ensured even illumination of the field. A push-button counter was available for recording of 6 different sizes of objects.

(4.5.2) The films used for optical photomicrography were Ilford HP_3 and HP_4, 35 mm film.

HP_4 was used because the straight portion in the H & D curve is in the useful range of densities for our purpose.

Figure (4.4) gives density against log. exposure for these films when they were developed in ID-II developer with intermittent agitation.

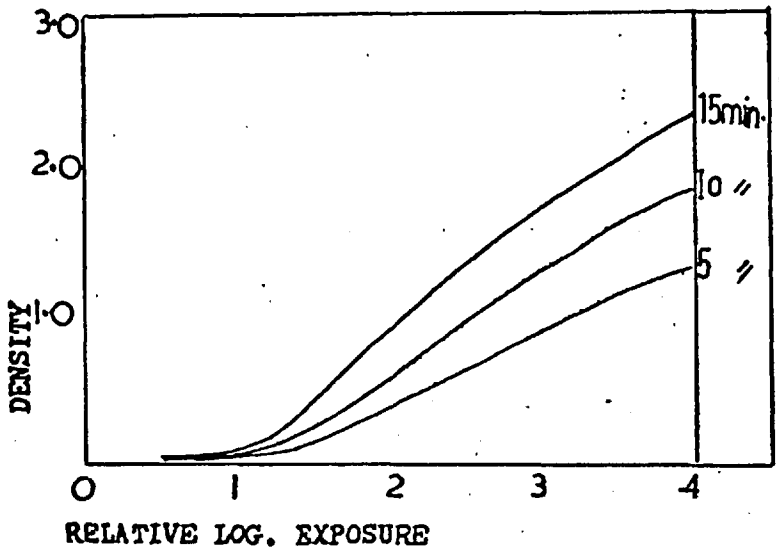


Fig. (4·4): H & D CURVES FOR H P 4 ILFORD FILM FOR THREE DIFFERENT DEVELOPMENT TIME .

For colour photography which was used only for qualitative purposes, Kodachrome 11 was used with speed rating of 40 ASA or 17 DIN.

(4.5.3) Electron microscope used: The transmission electron microscope used in this investigation for electron micrography of small reaction spots and for studying the traces of outdoor acid droplets on metal films is a "Siemens" electron microscope. The vacuum suitable for microscope operation is 10^{-4} torr. The focal length of its objective lens is 2.75 mm, and table (4.1) gives values of the angular objective aperture for two apertures:

internal diameter of aperture	angular objective aperture $x10^{-3}$ radian
50	9
5	0.9

Insertion of different objective apertures causes variation in resolving pewer and contrast on the final image screen.

Table (4.2) gives the limits of magnification obtainable in this electron microscope, which vary slightly with the H.T. voltage used.

Pole piece no.	mag. without intermediate lens on	mag.with intermediate lens on
1	1,000 x	8,000 x
4	18,400 x	160,000 x

Table (4.2) Limits of magnification on "Siemens" electron microscope.

The microscope operates with 60, 80 or 100 K.V. H.T. The higher voltage provides better penetration of electrons (increased velocity) and so makes it possible to study thicker specimens.

A holder for 12 plates (6.5 x 9 cm.) is inserted in the photographic chamber. A special drive brings individual plates into the field of exposure. The exposure shutter carries the viewing screen and both can be raised or lowered by turning a lever (full details in instruction and electron microscope hand books). For long period use of the microscope, liquid nitrogen is used to lower the temperature and prevent formation of contamination which decreases resolution on the image. The microscope final screen is circular, 9 cm. dia.

(4.5.4) Plates used for electron micrography and their calibration curve.

As a result of many experimental works, e.g. Barer and Cosslet (1966) or Hall (1967), it is known now that exposure of a photographic emulsion to electrons is almost entirely a single-hit process. Photographic plates used for recording electron images are plates without sensitizing dyes which are sensitive to electrons of all velocities but are insensitive to light of longer wavelength than the blue region. So they can be handled with enough light in the dark room. In processed plates the density (D = log (I/T)) is linearly related to the number of developed silver grains or in other words to the exposure (all these factors are fully described in the previous chapter). For the working densities usual in electron micrography, density is proportional to

to exposure. It can be written simply that where K varies from one emulsion to another D. = KE. We can conclude from plotted H & D curves for electrons that:

(E = exposure), $\gamma = \frac{dD}{d\log E} = 2.3E \frac{dD}{dE}$ (1)

where γ = slope of linear portion of curve so:

$\frac{dD}{dE} = K$, $D = KE \rightarrow \gamma = 2.3D$

From the above results one can say that the contrast of an emulsion exposed to electrons depends only on the density, and when exposed to the same density, all emulsions show exactly the same contrast.

Equation (1) is valid when $D \leq \frac{Ds}{4}$, where Ds is saturation density of plates.

Zeitler and Bahr (1959), who measured the mass density of an object by measuring contrast on electron micrographs, showed experimentall that these plates have a response such that plots of D against E have a portion which is linear to within 5% up to D = 1.5.

In this investigation, calibration curve of the plates was plotted for density against exposure (only time varies and intensity is kept constant). Density was measured with a "Joyce Loebl" microdensitometer.

The graphs were almost linear as expexted for these Ilford lantern contrast plates in the range of density measured.

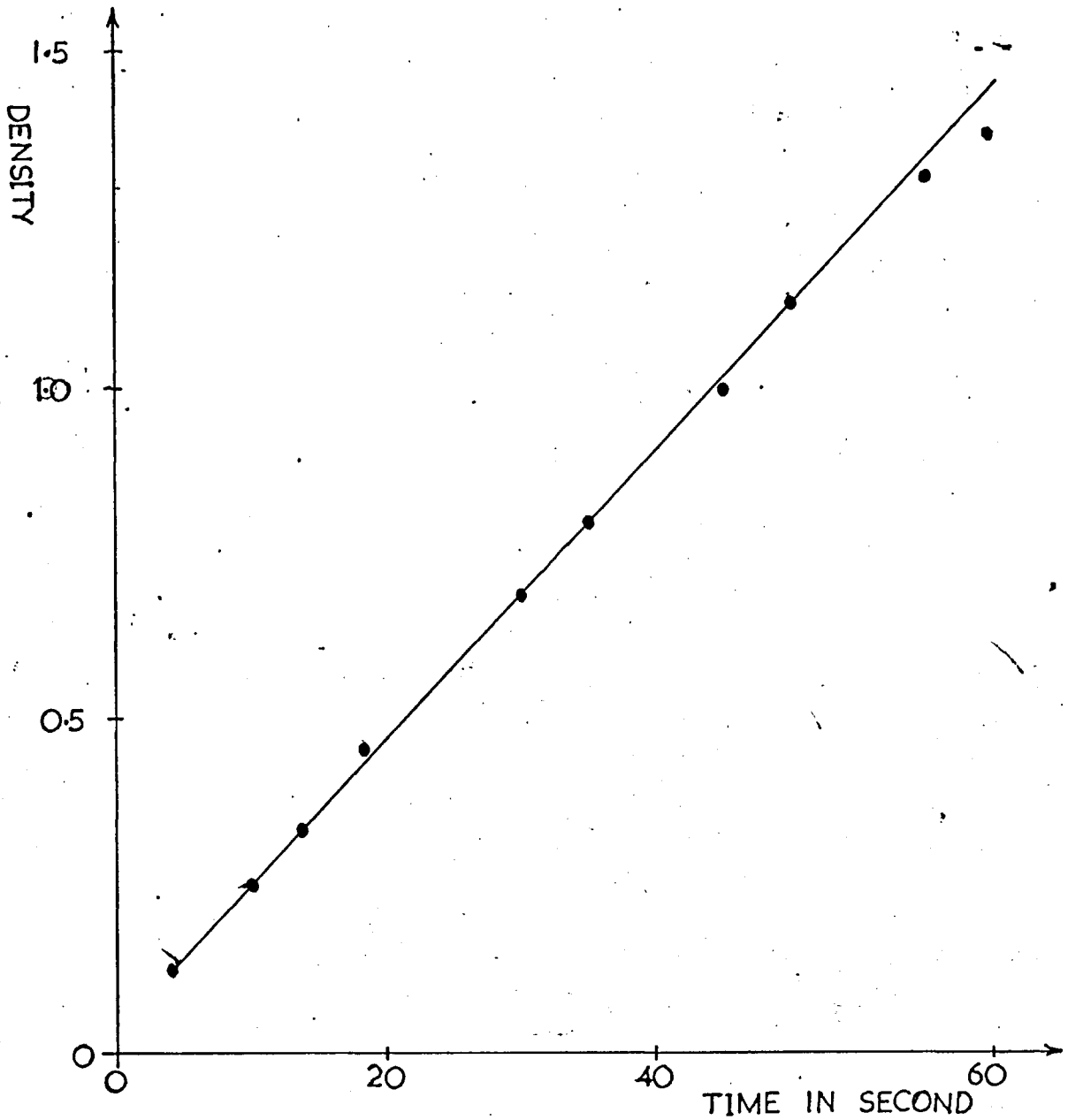


Figure ( ). Response of lantern contrast plate to standard densities

The graphs were almost linear as expected for these Ilford lantern contrast plates in the range of density measured.

(4.6) Preparation of thin metal films: In this investigation vacuum evaporated metal films were used. The vacuum system in which the films are prepared, is a high vacuum coating unit "Micro-BA3 Balzers". The vacuum system operates when the pressure falls to 10^{-5} torr. The voltage for the heating stage is 4,8 or 16 volts which corresponds to a current of 31, 62, or 125 amps. This causes evaporation of metal from the stage. Tungsten basket or wire is suitable suitable as a stage for high melting point metals and molyhdenum is used as evaporation stage for those of medium melting point such as copper. (Full details are given by Hall (1963)).

The best distance between substrate and stage is(10 - 15)cm. The thickness of the film can be roughly calculated from the length of metal wire evaporated. The substrate on which the metal film is formed is a glass slide (1" or 4/10") diameter .

The slides were cleaned by soaking them in fuming nitric acid and then adding isopropyl alcohol, which causes a slight explosion and removes all greasy materials. The slide is then washed thoroughly in distilled water and dried in a vacuum dessicator on a filter paper. The dried slide is then coated with a thin layer of Teepol of Formvar (This is done only when the thin film is going to be

studied with an electron microscope after exposure to acid drop). The layer then can be dissolved and the stripped metal can be released. The thin film of metal can be kept in a vacuum dessicator for about 24 hours, but it is much preferable if it is used and studied within a shorter period. When very thin iron film was coated with a thin layer of carbon, 150 A°, evaporated in the vacuum unit, which prevents cracking and damage to the film when stripping and releasing it from the substrate.(Exposed film).

For electron microscopy, the stripped film was caught on a grid support and thoroughly dried in a dessicator. It was found experimentally that wet metal films when exposed to electron beam were severely damaged and folded. It is useful to note that metal films thicker than 100 A° are supposed to have the same density as bulk metal.

(4.7) Development of technique: Among the metals exposed to acid droplets, iron and nickel showed regular reaction spots, i.e. the perimeter of the spots was nearly circular. These two metals have higher melting point than the others and have less mobility during the deposition of nuclei on the substrate, which gives the best chance of obtaining amorphous deposition. An amorphous layer was needed in this investigation for two different reasons:

a) An amorphous layer, or even a fine-structured layer gives reaction spots of a more regular form, which is desirable when the aim is merely to size the reaction spots.

b) Light absorption in a crystalline layer is a complicated problem, in which many factors such as crystal orientation and size are involved. But when the layer structure is quite fine, it can be regarded as an amorphous layer and light absorption obeys a very simple equation. For these reasons, a very fine structure was obtained by a technique of cooling the substrate and by using higher melting point metals such as iron and nickel.

The substrate was cooled to nearly -70 ^{o}C by putting the handle of its stage in liquid nitrogen for about one hour before deposition. By this device a very fine structure was obtained for iron film which even at 40,000 x magnification under the electron microscope shows quite fine amorphous structure. Figure (4.5) shows iron film deposited with a cooled stage under high magnification in the transmission electron microscope.

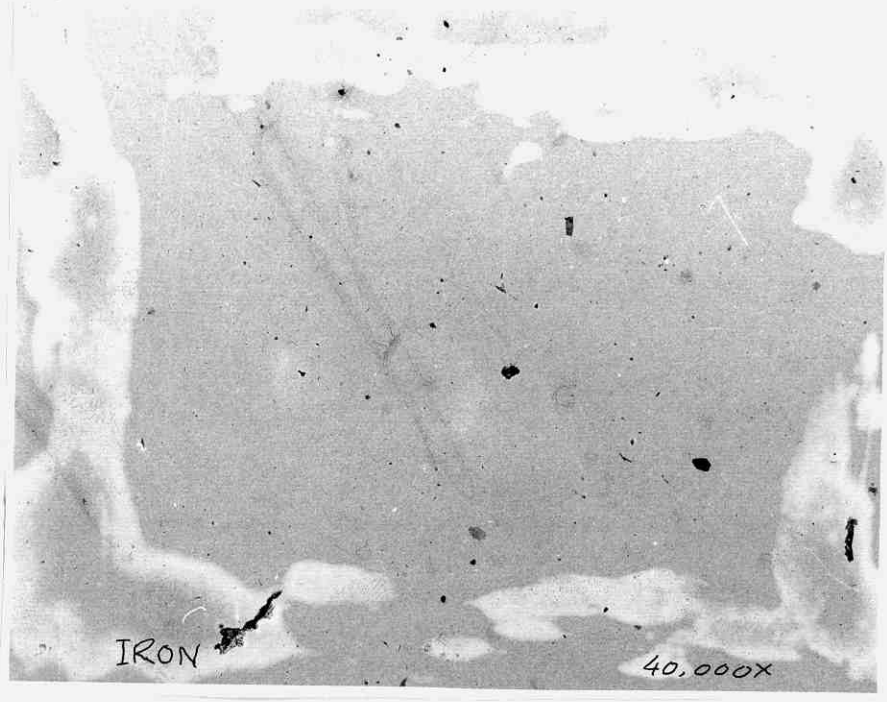


Figure (4.5).

The only problem which disturbed the cold stage method, and prevented the film from adhering properly to the substrate, was ice formation on the substrate. This happened because water vapour was not pumped out as completely as air from the vacuum unit. To prevent this ice formation, (P_2O5) phosphorous pantoxide was inserted in the vacuum chamber as a drying agent.

(4.8) Light Measurement through Spots: Iron films of different thickness were exposed to acid droplets of three different normalities or to outdoor pollution. The exposed film was kept in the vacuum dessicator for about one hour for completion of chemical reaction. It was then washed very carefully with distilled water and dried in the dessicater. The specimens were then studied under the optical microscope. The transparency of the field was measured using a photometer (exposure meter). The results of these measurements are tabulated and plotted in chapter 6.

(4.8.1) Photometer used: The photometer used to measure the light intensity through each field in the microscope is a Watson CDS exposure meter. This is an integrating meter measuring the total light energy over the field. It has a cadmium sulphide cell which can be fitted in place of the eyepiece of the microscope. It is designed to estimate exposure times for photomicrography. In this experimental work this exposure meter was used to measure the transmission of light through the individual fields. The photometer was first

calibrated using wedges with known standard densities. Graphs in figure (4.6) show the response of the cadmium sulphide cell plotted against density. Good straight lines were obtained for densities up to about 3.

(4.9) Photography through the optical microscope:

An EXACTA camera was fitted to the optical microscope and a set of photographs with a range of exposures was taken from each field using HP4 Ilford 35 mm. film. This was done only with the first set of photographs, in order to calibrate the exposure meter and to estimate a convenient exposure time for each brightness of field. The films were developed using ID-11 developer diluted (1+9) for a period of 9 minutes in complete darkness, and then fixed. Processed dried films then were studied in various ways. Although absorption by metal films represents the general type of absorption which is very nearly the same for all wavelengths, if the purpose of photography is densitometry through negatives, then a monochromatic source of light should be used, or an interference filter which provides a narrow range of wavelengths.

The extinction coefficient (fully described in the previous chapter) of metal film is measured by optical photomicrography of two different known thickness of the same metal. The density of the negatives gives the amount of light transmitted, and hence, k, the absorption coefficient, can be determined.

$$K = \frac{1}{2(t_2-t_1)\log e} \cdot \log I_{1/I_2}$$

and since $K = \frac{k\lambda}{2\pi}$, $\bar{k}$ can be derived.

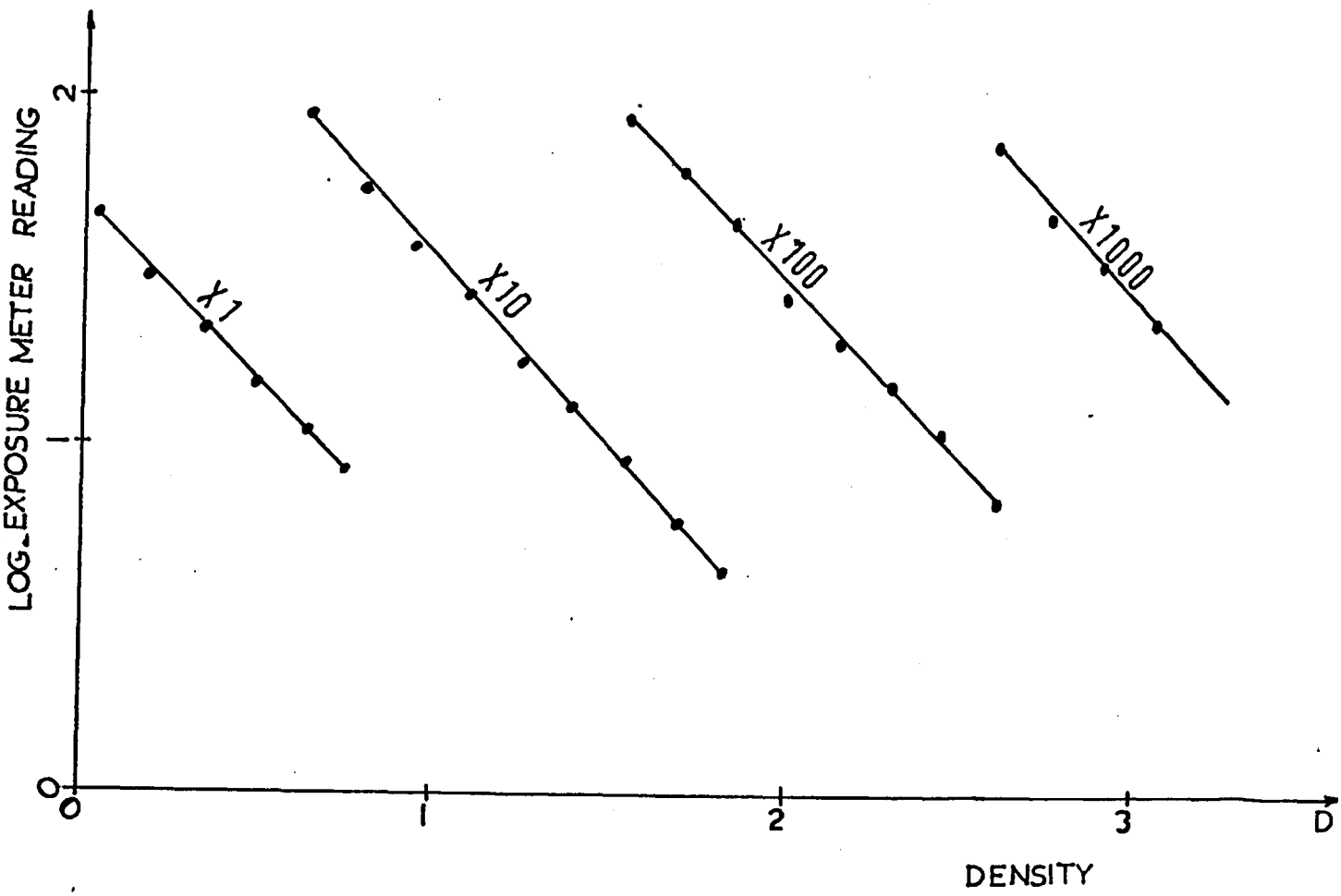


Figure (4.6) Log. Response of Exposure Meter Cell to Standard Densities

Care should be taken to ensure that the field is evenly illuminated and that the power supply for light system is sufficiently stabilized so that the intensity does not drift during the exposures. The image was carefully brought to focus before the photographs were taken.

(4.10) Photography through the electron miscrope:

When the desired image was seen on the viewing screen it was focused through a telescope and then the intensity was reduced (bias current reduced normally to 3 μA). A sensitive plate was driven underneath the screen and then an exposure was made, usually for a period of 5 seconds. The exposed plates were then processed with the same technique as for films. Dried plates were then used for density measurement. The effect of inelastic scattering on the final image can be disregarded because the angular apertures of objective was only about range of $ax10^{-3}$ radian. It has been experimentally proved (R.E. Burge (1960)) that in this range of aperture size, the effect of inelastic scattering is negligible. As mentioned in the theoretical section, for mass density ρt in range of (1-100) $\mu g/cm^2$, the contrast K is directly proportional to the mass thickness of the specimen. This corresponds to an iron film with thickness in the range (12 - 1200)A°. This shows that for the thickness and the metal used, density measurements from negatives can be converted accurately to contrast in the image plane which gives a fairly accurate estimate of the thickness of the metal film.

(4.11) Study of negatives from optical and electron micrography:

This is the method used to determine the depth of reaction pits on metal films exposed to acid droplets, and hence the volume of metal dissolved, and finally the equivalent weight of acid.

(4.11.1) In producing negatives, care was taken to illuminate evenly the whole viewing field of the microscope.

Fast films are unnecessary, and slower films are preferable because they give higher contrast. Films and plate development is very important. To obtain a uniformly developed negative, these steps should be taken: 1) Use of a considerable amount of developer in a large dish to minimize the risk of uneven development at the edges of plates.

2) Since the degree of agitation effects the degree of development, agitation should be given for a constant period and as evenly as possible, preferably not only in one direction.

3) The developer should be refreshed for each roll of film or set of plates developed.

It should be mentioned that because all the measurements for one set of results are done on one plate or negative, the above mentioned difficulties are mostly overcome and development is usually uniform enough over the whole plate.

(4.12) Instruments used for density measurement:

(4.12.1) Microdensitometer: A Joyce Loebl, microdensitometer was used for density measurement across the spots and for calibrating other systems used. Also this

Instrument is used for S_t measurement in electron micrography.

The films are fixed to the stage by a flat glass plate. The spot of light is moved across each spot or any interesting area in two or three different directions. The recorder gives the density across spots, point by point. The average density of each spot can then be calculated by using a planimeter to measure the area under the curve of density vs. distance.

The average density then yields the average intensity. This system is used for plotting calibration curves of plates and to calibrate also the densitometer which will be described later. The accuracy of density measurement with this microdensitometer is $\pm$ 0.014.

(4.12.2) Home made densitometer

This instrument has a tungsten iodide lamp fed by a power supply which provides a very stable and adjustable current and voltage through the lamp. The upper side of filament is used, which can be regarded as a point source of light. The light beam is converted to parallel beam by a well corrected short focal length camera lens and passes through a diffusing surface which gives a well scattered beam of light evenly covering the negatives. The light passing through the negative can be limited by a circular diaphragm and is collected by a photoconductive cell type ORP12. This is a cadmium sulphide cell for contrast and brightness control. Figure (4.7) shows the response i.e. output resistance of the cell against illumination (lux).

Figure (4.7)

The light passing through the whole area of the spot is focused on the surface of the sensitive cell by another well-corrected camera lens. The films and plate can be adjusted on a moving stage connected to a micromanipulator. The response of the photocell is detected by a digital multimeter which can resolve a resistance change of 100 micro-ohm. This densitometer is used to give the integral of density over the spot area, i.e. the total density of the spot. This then can be converted to average density for each individual spot. The system is calibrated using standard filters with densities (0 -3), (0-2) and (0.5 - 1) and Kodak step tablets.

The result of this calibration can be seen in figure (4.8). This shows that the response is linear within $\pm$ 0.1 for densities in the range (0-2.5).

This system is much easier to work with than microdensitometer and the results are easier to calculate. Although the home-made densitometer is not as accurate as the microdensitometer, its application is much easier when the spots are not quite regular.

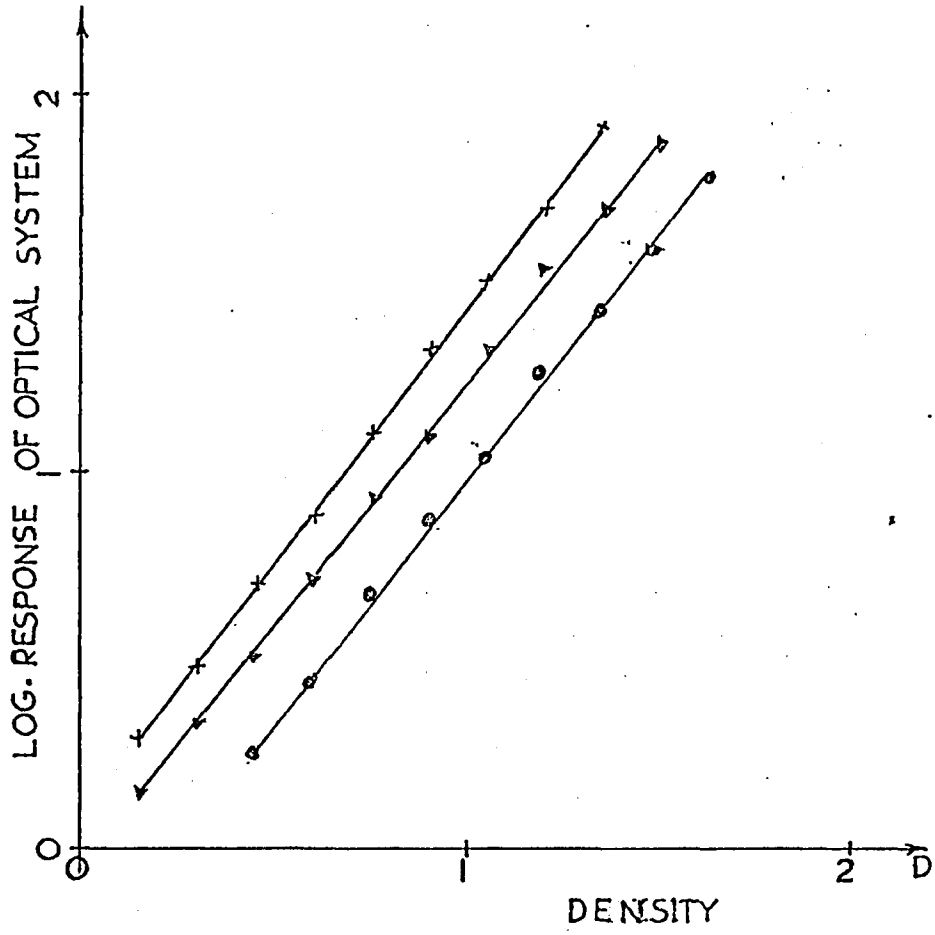


Figure (4.8) Calibration Curve for Home-Made Densitometer (Calibrated by use of Standard Filters).

The results of density measurement with this system from negatives of outdoor pollution sampled on iron was compared with density measured using the mocro-densitometer. The results agree within ±10%. This error is not entirely due to the response of the system but partly to non-uniform density of background of reaction spots when the microdensitometer was traversed in several different directions.

The accuracy of density measurement with this system is ± 10%.

(4.12.3) Flying spot used: Thds system is devised for measuring black spots on diffraction patterns. The magnification of the system is fixed but the size of the visible screen can be adjusted to cover the total area of spots. The meter reading is directly a measure of the total density of the spot. The instrument was used in this investigation for density measurements from negatives taken through the electron microscope from outdoors pollution samples. It has an accuracy equal to 10%. The results of these measurements are only used to be compared with results from the home-made densitometer.

CHAPTER 5.

THEORY OF METAL FILM TECHNIQUE FOR DETERMINING ACID PARTICLES

This chapter begins with two calculations showing that droplets of acid very rapidly reach equilibrium after a change in relative humidity, though they seldom collide with other particles in the air. The rest of the chapter presents a very simple theory of the metal film technique, illustrated by a series of calculations about several possible situations.

(5.1) Calculation on rate of evaporation of acid drpplets

The evaporation of very small droplets falling under gravity can be calculated as for stationary droplets. As illustrated by the calculation outlined below, droplets of sulphuric acid quickly reach equilibrium with the surrounding air.

In this calculation it is assumed that a 10 micron diameter drop of 2N acid entered a room with R.H. 50% and temperature 20 ^{o}C. The rate of evaporation is calculated from an equation quoted by Langmuir (fully described in section (3.1.2), using a stepwise procedure in which the drop diameter is reduced in increments of 1 micron.

The Zebel equation: $\frac{dr}{dt} = \frac{0.486}{r}\left(\frac{H}{100} - \frac{p_o}{p}\right)$

where H is R.H. indoors, r is in microns, and $\frac{dr}{dt}$ is in microns / millisec, is used to provide a numerical value for the rate of evaporation for comparison. Density and vapour pressure of the acid drop at each step is calculated from its volume and weight. The results of these calculations are given below:

1) From Langmuir equation:

$$\frac{2N\text{acid } r_o = 5}{\text{drop}} \text{ to } \underline{45\% \text{ acid } r = 2.6} \quad \text{in } \theta = 0.066 \text{ sec}, \; x = 0.0132 \text{ cm.}$$

2) From Zebel equation:

$$\frac{2N\text{acid } r_o = 5}{\text{drop}} \text{ to } \underline{45\% \text{ acid } r = 2.6} \quad \text{in } \theta = 0.069 \text{ sec.}, \; x = 0.0134 \text{ cm.}$$

It can be seen from these results that the drop evaporated from the initial concentration of 2N(10%) to nearly 45% in only 0.066 or 0.069 sec. The diameter decreased to 2.6 μ. During this process the drop would have fallen (0.0132 or 0.0134) cm.

The conclusion of these calculations is that acid droplets need only a fraction of a second to evaporate to a rather strong acid when they enter indoors. But fortunately during the period of respiration, in respiration system where R.H. is very high they soon get diluted and less harmful.

(5.2) Calculation on deposition of small solid particles on acid drop (i.e. collision of drop with small solids):

The rate of increase in mass of a droplet, due to deposition or collision of very small solid particles, is now calculated.

$$\frac{dm}{dt} = 4\pi D m_2 C_o r$$

where $\frac{dm}{dt}$ rate of growth of drop by adding small solid. D = diffusion coefficient for 0.2 μ diameter particle $= 2.2 \times 10^{-6}$. m_2 = mass of solid particle (ρ assumed to be 1.5 g/cm^3). C_o = concentration of particles indoor, assumed = 5700 par/cm^3, r = radius of drop = 1 μ $= 1 = 10^{-4}$ cm, t = time for one solid particle to collide with acid droplet.

$$\int_o^{m_2} dm = 4\pi D m_2 C o r \int_o^t dt, \text{ so } t = 17 \text{ hrs. } 40 \text{ mins.}$$

hour

Another version of this formula is quoted by Smoluchowsky, giving the number of solid particles which can be removed by an acid drop with radius r '

$$\frac{dn}{dt} = 4\pi DSn_o.$$

With the same assumptions as before, and taking t = 17 hours 40 minutes, then n ¼ which means that a long period of time is needed for an acid drop to collide with a small solid particle. But since 80% of outdoor acid droplets do contain solid particles, it can be concluded either that the concentration of solid particles in air is far greater than was assumed, or that this is mostly due to condensation of acid on (usually hygroscopic) solid material.

Introduction to theory of metal film technique

Though several workers have tested this method experimentally, it seems that the theory has never been considered at all. It is therefore necessary to work out a simple theoretical basis for the method. This theoretical section is brought in to fulfill three purposes:

1. To illustrate and explain the principles involved.
2. To provide a basis for quantitative or at least semiquantitative calculations.
3. To show the limitations of the method, which is probably the most important purpose. Even with the simplest theory, it can be seen that large errors are likely to occur in certain kinds of estimation. It is not certain that this theory always applies even for acid particles which have no solid in suspension. Therefore,

for simplicity, assumptions are made to make theoretical calculation possible in each case. These assumptions are not necessarily exact and the simplest possible conditions are assumed. The basis of the theory is simply that the acid in each droplet dissolves, and in effect removes, the equivalent amount of metal. This makes a (shallow) pit, and increases the light transmission.

In all cases, the acid content of the droplets is used to calculate the volume of the pit that is formed when the droplet reacts chemically with a thin metal film.

By assuming a ratio of spot (i.e. pit) diameter to drop diameter, the depth of the pit formed is calculated. The difference in transmission of light or electrons through the spot and through the background of unaffected metal film is estimated with the assumption that the exposed film is studied under an optical or electron microscope.

The validity of the assumptions, and the conditions under which they are likely to hold, are discussed in the light of experimental results in the next chapter. In all calculations about light transmission, the pits are assumed to be cylindrical on average and the metal is supposed to be an ordinary absorbant layer for light transmitted through it.

(5.3) Calculation of diameter of reaction pits in copper and the possibility of holes as the result of chemical reaction.

In this set of calculations, the possibility of having holes all through the metal film is discussed.

Assumptions: 1) aerosol = 4μ diameter 2N sulphuric acid.

2) metal = copper.

3) $cu + \frac{1}{2} O_2 + H_2SO_4 \rightarrow CuSO_4 + H_2O$

4) 63.5 g cu $\equiv$ 98 g. H_2SO_4.

5) D = drop diameter and d = reaction spot diameter.

From the mass of copper which is dissolved in acid by the above chemical reaction, the mass and the volume of the reaction pit can be calculated assuming the depth of the pit to be equal to the metal thickness. General relations are given below :

In next page

Table (5.3.1) Effect of a 4 μ^{l} Sulphuric Acid Droplet on Copper with Different Thicknesses.

Table (5.3.1) Effect of a 4μ Sulphuric Acid Droplet on Copper with Different Thicknesses

Thickness of metal film A°	Diameter of reaction hole μ	Reaction hole dia. / Drop dia.
(1) 10% acid drop		
200	4.10	1.02
300	3.36	0.84
400	2.92	0.73
500	2.62	0.65
800	2.06	0.51
1000	1.84	0.46
(2) 45% acid drop		
200	9.92	2.50
300	8.10	2.02
400	7.11	1.80
500	6.34	1.60
800	4.98	1.24
1000	4.45	1.11
(3) 100% acid drop		
200	16.60	4.15
300	13.61	3.40
400	11.82	3.00
500	10.60	2.65
800	8.34	2.08
1000	7.45	1.86

between D and d for three different concentrations of acid drop:

1) 10% acid drop: $d^2 = 0.53 \times 10^{-2} \frac{D^3}{h}$

2) 45% acid drop: $d^2 = 3.1 \times 10^{-2} \frac{D^3}{h}$

3) 100% acid drop: $d^2 = 8.67 \times 10^{-2} \frac{D^3}{h}$

Here h is assumed to be the thickness of copper film and d is calculated. Table (5.3.1) shows results of these calculations for different thickness of copper film.

It is unlikely that the diameter of the reaction spot will be smaller than the diameter of the acid droplet, so, for a 4 μ, 2N acid drop it is only on 200 A^{O} copper that the reaction pit can possibly be a hole all through the copper film. But for more concentrated acid droplets, such as 45% or 100% for the same drop size the hole may go right through, even with films much thicker than 200 A^{O}.

(5.4) Calculation on light transmission through unexposed iron films: Because most of the experimental work and calculations were done using iron films in this investigation, iron films are chosen to illustrate the calculation of transparency and its variation with thickness.

Assumptions: for $\lambda = 5890$ $\bar{n}\bar{k} \approx 3.4$ (derived from Drude tables)

and so $K = \frac{4\pi\bar{n}\bar{k}}{\lambda} \approx 70$

(λ is in micron)

The light absorption equation is fully described in sections (3.5.5), (3.7.2) and (4.9). Symbols have the same meanings. Table (5.4.1) shows the result of these calculations:

Iron thickness A^o	$(T = \frac{I_B}{I_o})_{\%}$	log (%T)
200	24.6	1.39
250	18.0	1.25
300	12.2	1.09
350	8.5	0.93
400	6.0	0.78
450	4.5	0.65
500	3.0	0.48

Table (5.4.1)

As can be seen, iron films thicker than 500 A^o are nearly opaque.

(5.5) Calculation on light transmission through reaction pits in iron films with different thicknesses when exposed to to acid drops with three different concentrations.

Assumptions:

1) Drop diameter = 1 μ
2) Spot diameter = 2.5 μ
3) Aerosol is 10% or 45% (by weight) sulphuric acid.

4) Metal is iron.

5) Thickness range of iron = (200, 400, 500, and 600) A^{o}.

6) Metal absorption coefficient K = 70.

7) Original intensity of light = I_o.

8) Reaction pits are cylindrical with depth equal to h.

Referring to simple chemical reaction between acid and iron (mentioned in section (5.7)), dissolved iron due to reaction of acid drop of either concentration is simply calculated. Replacing numerical values in this equation gives two rather general equations relating spot diameter, drop diameter and depth of pit formed.

a) For 2N. acid on iron,

$$0.0323 \times D^3 = 6.16 \times h \times d^2$$

symbols have their usual meanings and units (of h, d and D) must be the same.

b) For 45% acid on iron,

$$0.177 \times D^3 = 6.16 \times h \times d^2$$

Using above equations depth of pits formed can be calculated. The light absorption equations then provide the relative increase in intensity of pits in any case. Transmission $T = \frac{I_s}{I_o}$ then results, in table (5.5.1) and Figure (5.5.1).

NORMALITY OF ACID DROP	THICKNESS OF IRON FILM	$\left(\frac{I_s - I_B}{I_B}\right)\%$	$\left(T = \frac{I_s}{I_o}\right)\%$	LOG. T
10 %	200	5.9	27	1.43
〃	300	1 〃	13	1.139
〃	400	〃	6.4	0.806
〃	450	〃	4.57	0.66
〃	500	〃	3.14	0.497
45 %	200	36.7	34.5	1.538
〃	300	〃	16.5	1.21
〃	400	〃	8.8	0.94
〃	450	〃	6.	0.78
〃	500	〃	4.18	0.60
100%	200	159.5	81.6	1.912
〃	300	〃	38.6	1.589
〃	400	〃	16.2	1.21
〃	450	〃	11.5	1.06
〃	500	〃	8.4	091

Table (5.5.1) Relative increase in light.intensity and T for reaction spot of a 1 M acid droplet on iron.

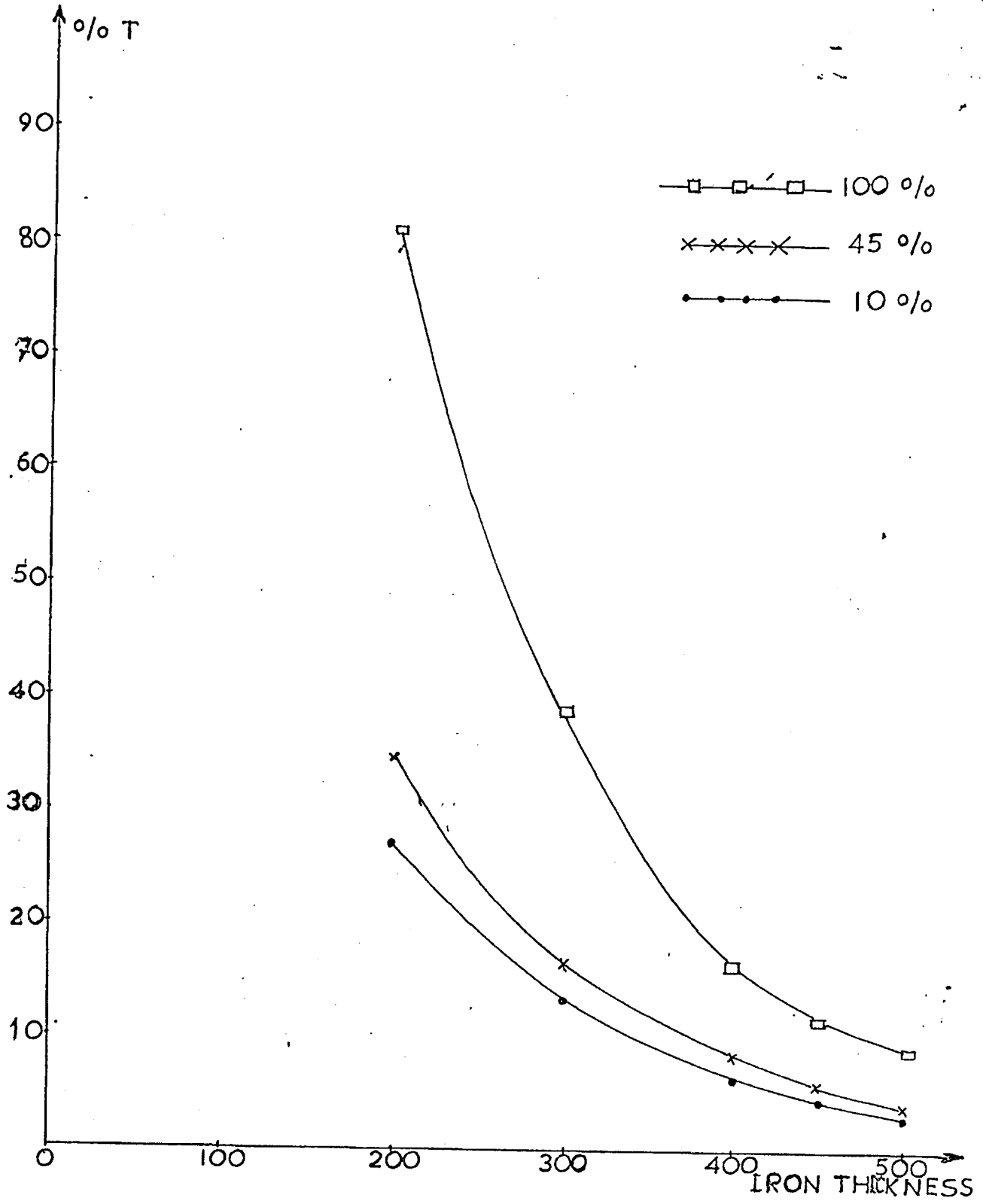


Figure (5.5.1) % T for a 1 μ acid reaction spot on iron films against thickness of iron

(5.6) Calculation on light transmission through metal film exposed to acid droplets of a range of diameter and concentration.

Assumptions: 1) Diameter of acid drop is (0.5, 1.0, 1.5, 2.0 and 5) μ .

2) Spot diameter is 1.4 and 2.5 times drop diameter.

3) Metal is 500 A^{o} thick iron.

4) Aerosol is 10%, 45% and 100% sulphuric acid drop.

5) Wavelength of light used in optical microscope is 5890 A^{o} (sodium).

The same type of calculation done in section (5.5) is carried out in this section to determine the percentage increase of light transmission through different spots due to reaction between iron and sulphuric acid droplets. Numerical values of densities, rate of concentration and atomic weight of acid and iron, gives the three following relationships between d, D and h.

1) For 10% acid: $h = 5.24 \times 10^{-3} \times \frac{D^3}{d^2}$

2) For 45% acid: $h = 28.7 \times 10^{-3} \times \frac{D^3}{d^2}$

3) For 100 Acid: $h = 87.1 \times 10^{-3} \times \frac{D^3}{d^2}$

In each case, for a cylindrical pit the relative increase in light transmission can be calculated using Bouguers equation for light absorption. Results are tabulated in tables (5.6.1) and (5.6.2).

From this table, it can be seen that in case of d/D = 1.4, a droplet 5 μ diameter of 45% acid, or a droplet bigger than 1 μ diameter of pure acid make holes

Table (5.6.1) Relative increase and % transmission of light through reaction spots on 500 A^{O} iron when d/D = 1.4

D Drop dia. μ	h Depth of pit A^{O}	$(\frac{I_S - I_B}{I_B})$ %	% T = $(\frac{I_S}{I_O})$ %
	10% acid drop		
0.5	12.9	9	3.3
1.0	25.9	20	3.6
1.5	38.9	31	3.9
2.0	52.1	45	4.4
5.0	129.6	145	7.36
	45% acid drop		
0.5	70.3	63	5.0
1.0	140.5	165	8.2
1.5	210.8	331	13.5
2.0	291.4	654	25.5
5.0	-	-	-
	100% acid drop		
0.5	222.5	367	15.4
1.0	445	1261	63.4
-	-	-	-

Table (5.6.2) Relative increase and transmission of light through reaction spots on 500 A^{o} iron when d/D = 2.5

D Drop diameter	h Depth of pit A^{o}	$\left(\frac{I_S - I_B}{I_B}\right)\%$	$T\% = \left(\frac{I_S}{I_o}\right)\%$
	10 % acid drop		
0.5	4.1	2.7	3.2
1.0	8.2	5.8	3.3
1.5	12.2	8.8	3.5
2.0	16.3	11.9	3.7
5.0	40.6	32.4	4.1
	45% acid drop		
0.5	22.0	16.4	3.6
1.0	44.1	36.7	4.3
1.5	66.1	58.1	4.9
2.0	88.0	84.1	5.7
5.0	220.3	394.3	14.2
	100% acid drop		
0.5	69.0	61.2	5.0
1.0	139.1	159.5	8.4
1.5	209.0	325.6	13.6
2.0	279.2	568.6	22.5

all through an iron film 500 A° thick. But if d/D = 2.5, this condition occurs only for a 5 μ drop of pure acid.

(5.7) Calculation on transmission of light through a field of 1,000 spots:

This calculation illustrates the estimation of the total weight concentration of sulphuric acid in air. This can be done by measuring the transparency or total light energy which is transmitted through a field containing e.g. 1,000 spots or in other words reaction pits. The spots are not measured individually, but the whole field of view in the microscope is used for light intensity measurement. This field is then compared with an unexposed field.

Assumptions:
1) Light transmission difference is only due to thinning of metal films on spot areas.
2) Drops of acid are all the same size.
3) Spots on iron film are all the same size.
4) Spot diameter is 1.4 times drop diameter.
5) Acid drop is 10% or 2N acid.
6) Visual area of one field = 346×10^{-6} cm^2.
7) Energy E = I x S (intensity x area).
8) $Fe + H_2SO_4 \rightarrow FeSO_4 + H_2\uparrow$

Referring to the above chemical reaction, the volume and depth of the reaction pits are calculated. By using light absorption equation (fully described in the last chapter) and by assuming energy to be the product of intensity and total spots area, the relative increase in energy is calculated for each field of 1,000 spots.

E_B = total field aread $\times I_B$.

$\Delta E = (I_S - I_B) \times$ total spots area.

% relative increase in energy = $\frac{\Delta E}{E_B}$ %

Total energy transmitted after exposure = $E_B + \Delta E$.

In table (5.7.1), the results from these calculations are given for different diameters of acid drop. C.G.S. units are chosen in all these calculations.

The table (5.7.1) is tabulated on the next page.

Drop diameter μ	Spot diameter μ	Depth of pit A°	Total Spots area $\times 10^{-5}$ cm.	Spots area / Total field area	% $\left(\frac{\Delta E}{E_B}\right)$
0.5	0.7	13	0.385	1.1	0.1
1.0	1.4	26	0.785	2.0	0.4
1.5	2.1	39	1.767.	5.1	1.5
2.0	2.8	52	3.142	9.0	4.1
5.0	7.0	130	19.635	56.0	82.7

Table (5.7.1) Relative increase of energy for light transmitted through a field of 1,000 spots.

(5.8) Calculation of the smallest drop of 2N sulphuric acid which can be detected by this method.

This calculation is done to work out the sensitivity of system for detecting acid droplets.

Assumptions: Metal = iron

Aerosol = 2N sulphuric acid drop

$\frac{dI}{I}$ = 3% is detectable (for spot to be seen on background).

$\frac{dI}{I}$ = 3% gives Δt (thickness different) = $4.2A^{o}$

0.5 μ diameter = smallest possible spot which can be seen with optical microscope.

From these assumptions the volume of the smallest detectable fit is calculated and hence the acid content of the drop. Assuming the acid is 2N gives the volume, and therefore the diameter, of the smallest drop that can be detected by this method.

Mass of iron dissolved = 6.15×10^{-16} g.

Mass of equivalent acid = 10.95×10^{-16} g.

Volume of 2N acid drop = 9.95×10^{-15} cm^3.

D = diameter of 2N acid drop $\simeq$ 0.3 μ

The conclusion from this calculation is that by studying either individual reaction pits by an optical microscope or by studying negatives from photomicrographs, it is possible to detect a drop of 0.3 μ diameter 2N acid, or in other words 10^{-15} g acid by this method. A much smaller quantity can be detected using an electron microscope (see chapter 6).

(5.9) Estimate of error in determining acid content from measurements of light transmission through film.

If the method were completely accurate, then a given amount of sulphuric acid should always produce the same increase in light transmission. In other words, a given amount of acid should always produce the same effect in terms of the product of spot area times increase in light transmission. However, since light transmission is governed by an exponential equation, and absorption is not linearly proportional to thickness of film, error increases as the reaction pits increase in depth. The calculation of pit depth has already been discussed: in the calculations that follow it will be assumed that the method is accurate for a 0.5 micron drop of any concentration. The results are expressed by giving the error that will arise for any larger drop size. This error is always positive, i.e. the amount of acid is over-estimated if the drops are larger than the 0.5 micron assumed. Numerical values are given in table (5.9.1).

The conclusion from results of these calculations is that, the method looks to be quite satisfactory ($\pm$ 10%) for 2N acid droplets up to 2μ diameter. For much stronger acid or very large droplets, the significance of method decreases rapidly, but these conditions are unlikely in work on air pollution. Even in these cases, it is possible to reduce error of size measurement by increasing the spread of the droplet on the metal surface or in other words by increasing the ratio of spot diameter to drop

Table (5.9.1): Errors of acid droplet size measurement using light transmission method for two different spot dia. on 500A° iron

Drop dia.	Spot dia.	$\frac{I_S - I_E}{I_B}$	$As(\frac{\Delta I}{I_B})$ / vdrop	% error
		2N	Acid Drop	
0.5	1.25	0.0266	4.988×10^3	0
1	2.5	0.0578	5.420×10^3	8
1.5	3.75	0.0882	5.512×10^3	11
2.0	5.0	0.1194	5.560×10^3	12
5.0	12.0	0.3243	6.081×10^3	41
		45%	Acid Drop	
0.5	1.25	0.1641	30.77×10^3	0
1.0	2.5	0.3672	34.44×10^3	12
1.5	3.75	0.5812	36.33×10^3	18
2.0	5	0.8408	39.13×10^3	27
5.0	12.5	3.9431	73.8×10^3	140
		2N	Acid Drop	
0.5	0.7	0.088	5.18×10^3	0
1.0	1.4	0.196	5.76×10^3	10
1.5	2.1	0.309	6.057×10^3	17
2.0	2.8	0.4515	6.381×10^3	23
5.0	7.0	1.4553	8.557×10^3	65
		45%	Acid Drop	
0.5	0.7	0.626	36.84×10^3	0
1.0	1.4	1.648	48.46×10^3	31
1.5	2.1	3.310	64.89×10^3	76
2.0	2.8	6.530	92.29×10^3	150
5.0	7.0	-	-	-

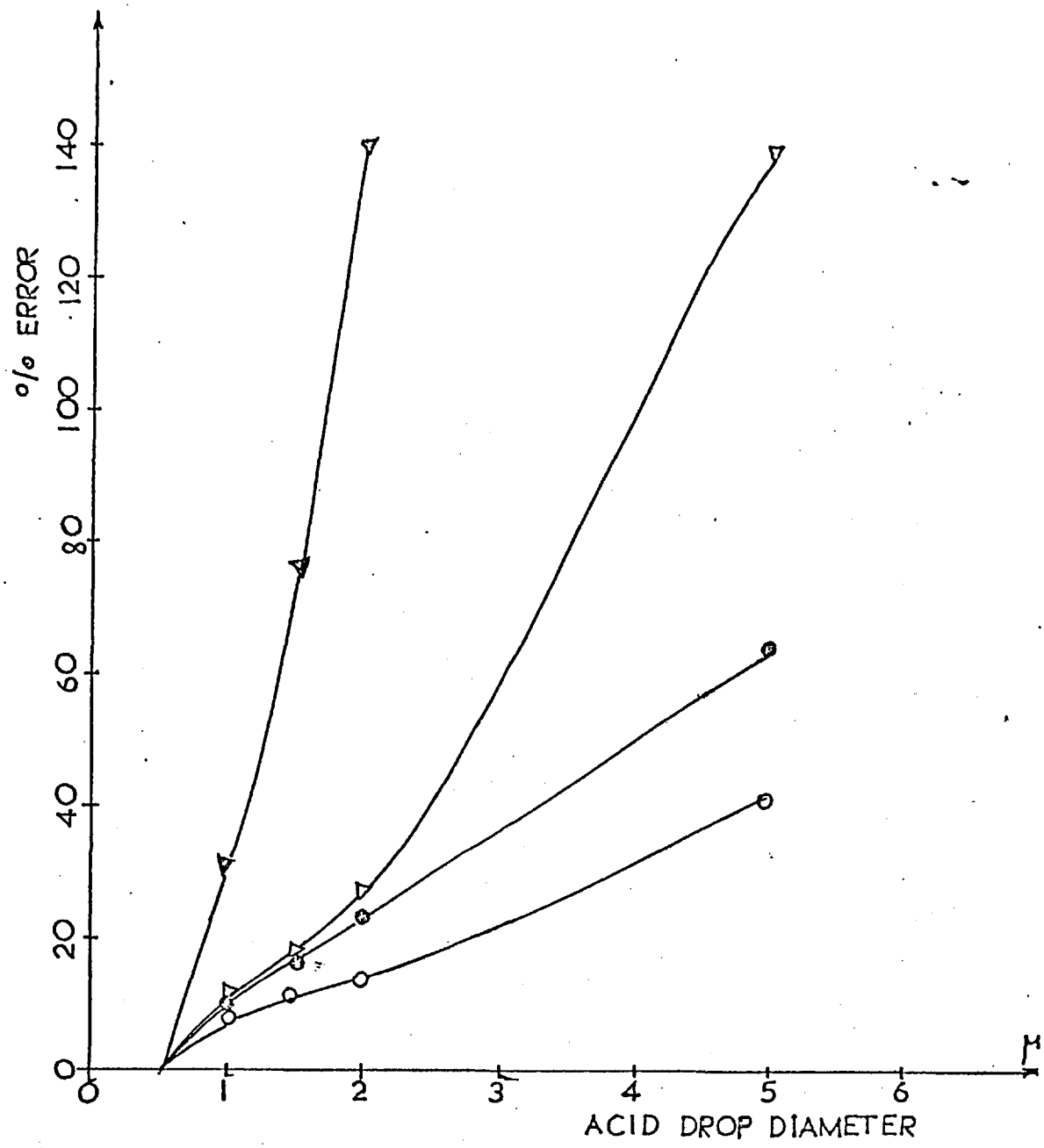


Figure (5.9.1) % of error on estimating size of acid droplets (sulphuric acid on iron). ▲–▲–▲–, ●–●–● for d/D = 1.4 and ▲–▲–▲– ○–○–○ for d/D = 2.5.

diameter. For pure sulphuric acid this method is applicable only to very small drops. But because the normality of atmospheric sulphuric acid droplets does not exceed 10% or 2N, so, theory suggests that within $\pm$ 10% accuracy (or even less for submicron droplets of acid which are the major part of atmospheric acid), the method can be applied for size and concentration measurement.

CHAPTER 6

RESULTS AND DISCUSSION

(6.1) Qualitative studies of metal films exposed to acid drops At the start of this investigation, vacuum evaporated metals - silver, copper, iron and nickel - were exposed to acid droplets from an ordinary sprayer. It was found that each metal shows a characteristic pattern in the reaction spot which differs from one metal to another. Though Schechter relates surface reaction to the fine structure of the evaporated metal, the reason for the quite regular pattern such as can be seen on nickel is not fully understood. Figures (6.1), (6.2), (6.3) and (6.4) represent reaction spots on different metals when exposed to acid droplets. Silver shows rather irregularly shaped reaction spots, though quite characteristic even for very small spots studied by stereoscan electron microscope, Figure (6.5). Copper has a rather coarse crystalline structure which causes completely irregular reaction spots (Figure 6.3) and (6.6). When metal is evaporated onto a cold stage substrate as described in the last chapter, the fine grain structure of the metal produces relatively simple and regular reaction spots. As can be seen in Figure (6.7), the reaction spots look quite circular and regular pits, in line with the theory described.

Figure (6.8) shows a condition which occurs only when a very thin (200 A^{o}) film is exposed to acid mist and then studied with an electron microscope. The metal has folded back from the light area in the centre, producing the surrounding dark patches. It is not certain whether this folding occurs during chemical

All figures in negative form.

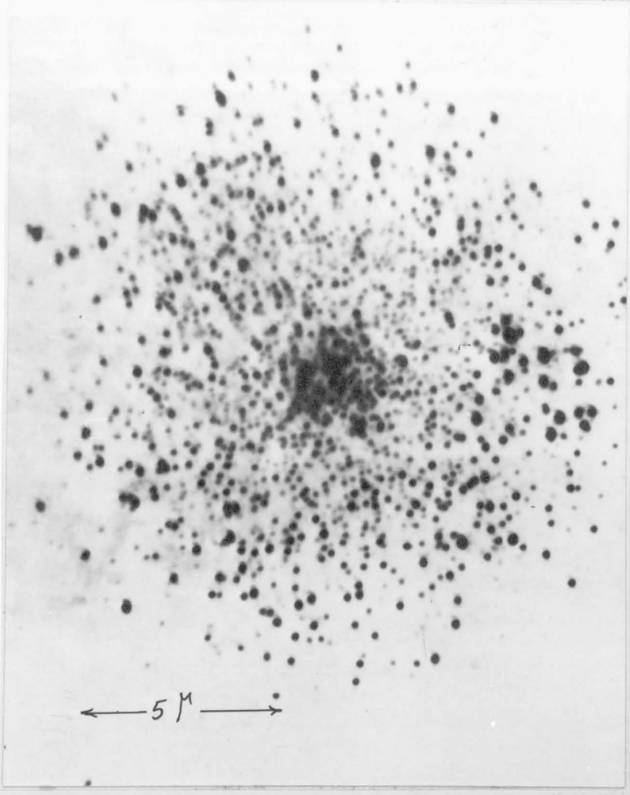


Figure (6.1) Reaction spot of 2N acid on silver.

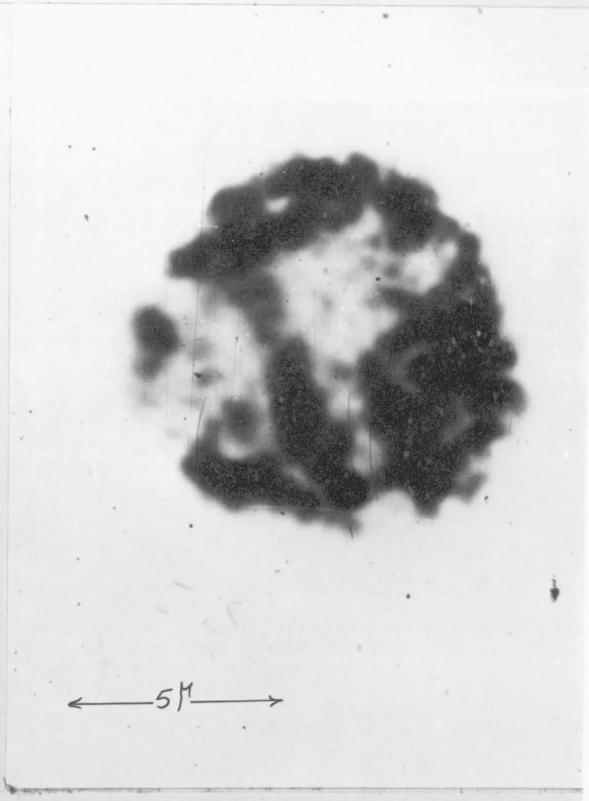


Figure (6.2) Reaction spot of 2N acid on copper.

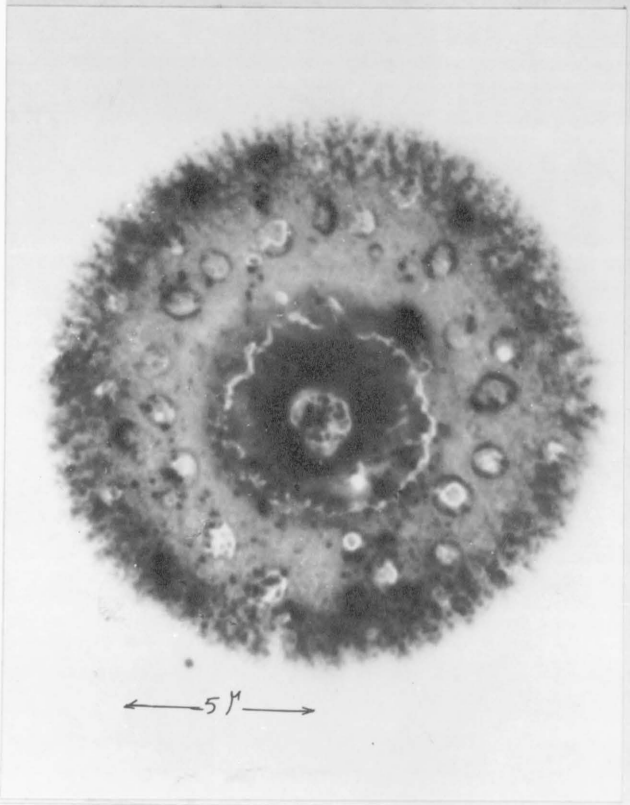


Figure (6.3) Reaction spot of 2N acid on nickel.

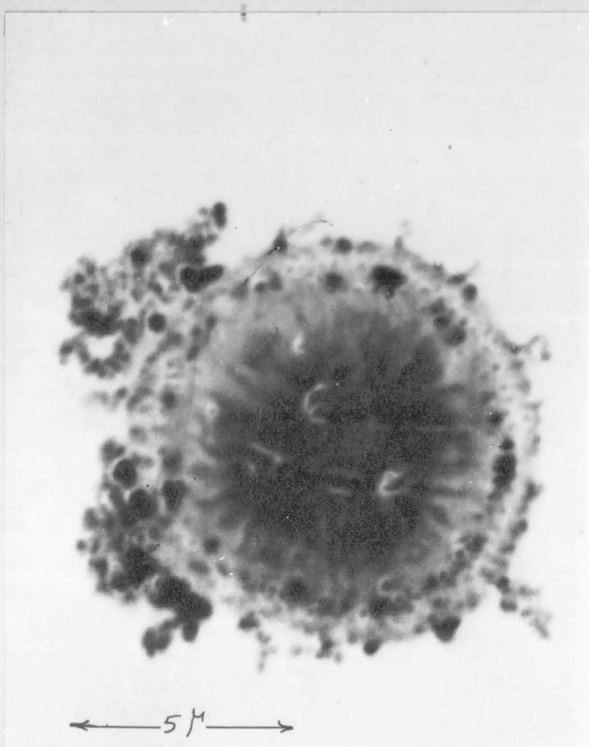


Figure (6.4) Reaction spot of 2N acid on iron.

reaction or during exposure to the electron beam. It can be usually avoided either by using thicker films, or if a thin film is needed, by coating the exposed metal film with a thin layer of carbon.

In some cases when the drop begins to react immediately when it is deposited on the metal film, a bright ring appears near to the perimeter of the droplet and then becomes wider for a few seconds after deposition. Then a pattern appears suddenly in the spot. Figures (6.A) and (6.B) show this happening when a droplet reacts with a metal film and (6.C) represents microdensitometric traverse of this type of spot.

In some other cases when reaction occurs, the resulting pit is rather regular, but instead of a clear ring, it is surrounded by a more opaque area. This condition can be seen in Figure (6.D) which is taken from such a pit using the scanning electron microscope.

(6.2) Sizing reaction spots: When the reaction spots are regular in shape and mostly circular, their size may be related to the sizes of the acid drop, as found by other investigators.

To study this, sulphuric acid mist of the desired concentration and acid percentage was made with the Devilbiss ultrasonic nebulizer. The mist was exhausted and diluted with oxygen-free nitrogen. Free-falling acid drops were sampled on a 100 μ silicone layer and on a 250 A^{o} nickel-coated slide in the sampling stage as explained in Chapter 5.

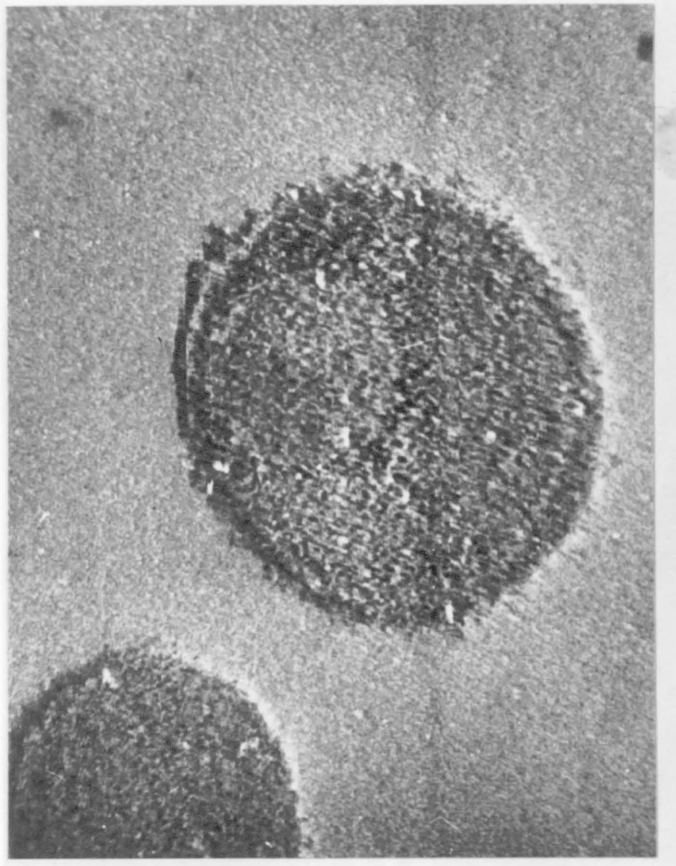


Figure (6.7) Reaction spot of 2N acid on iron with fine grain structure.

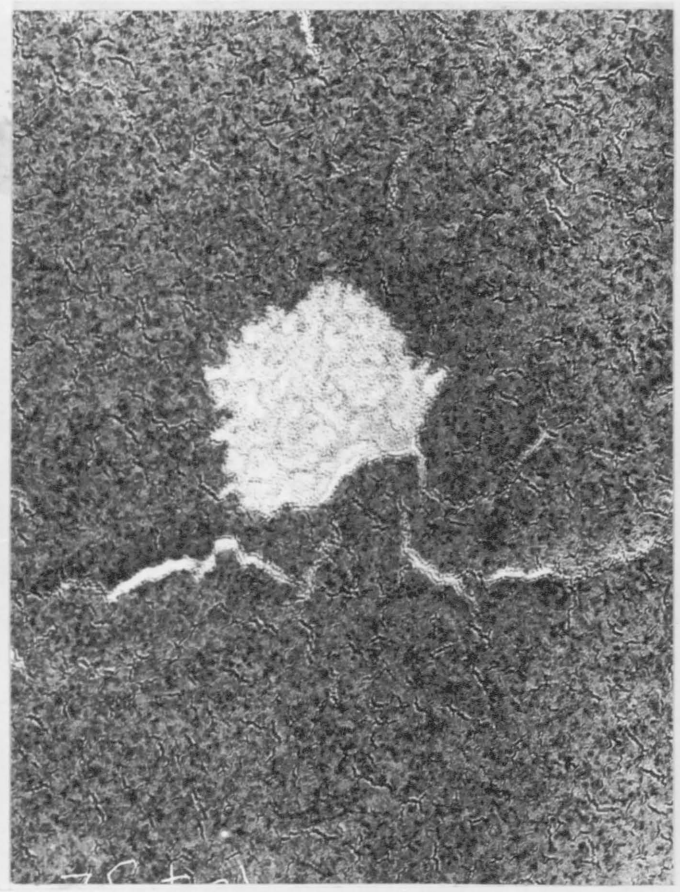


Figure (6.6) Reaction of 2N acid on copper (electron micro-photograph).

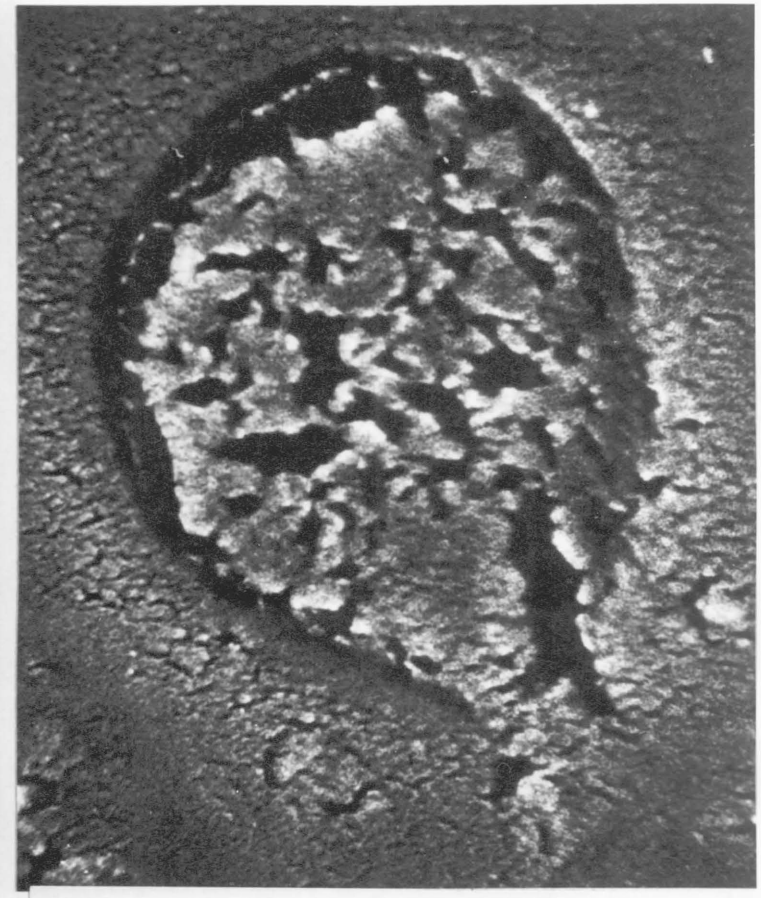


Figure (6.5) Reaction spot of 2N acid on silver (scanning electron micro photograph).

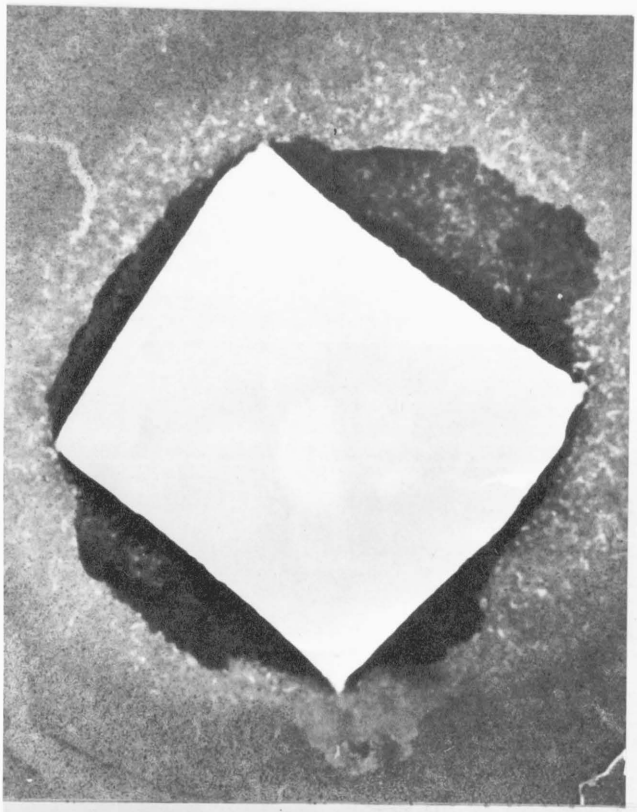


Figure (6.8) Irregular reaction spot of 2N acid on thin iron film.

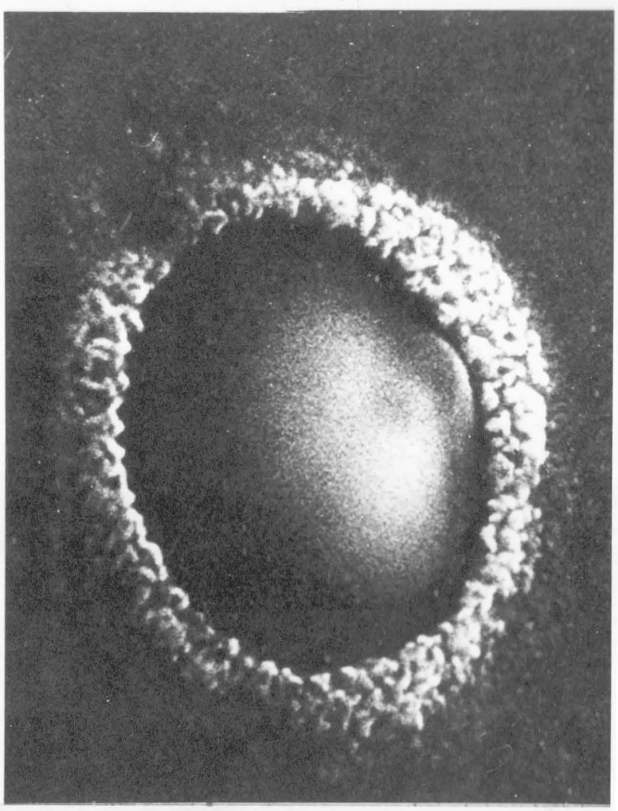


Figure (6.D) Scan electron micrograph of reaction spot with thicker perimeter.

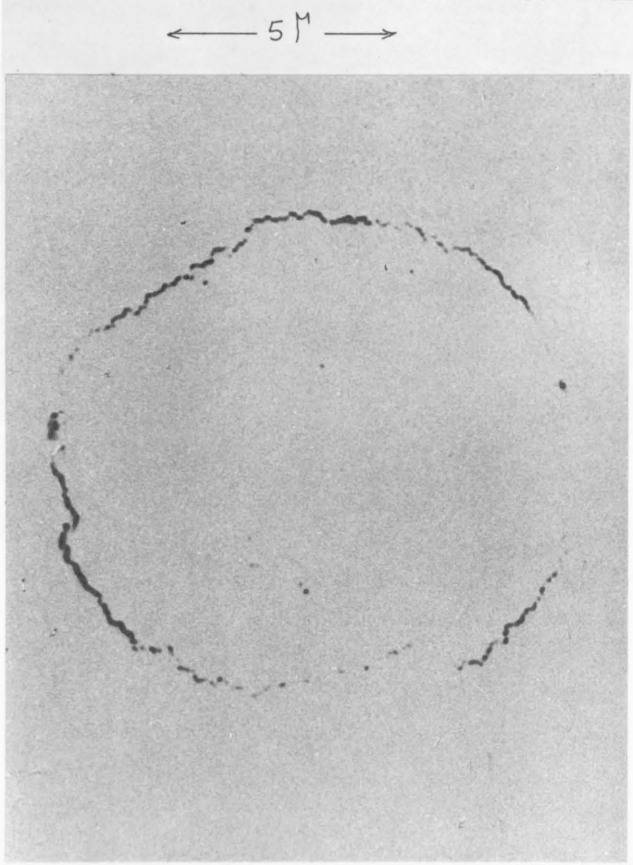


Figure (6.A) First section of appearance of reaction spot on iron film.

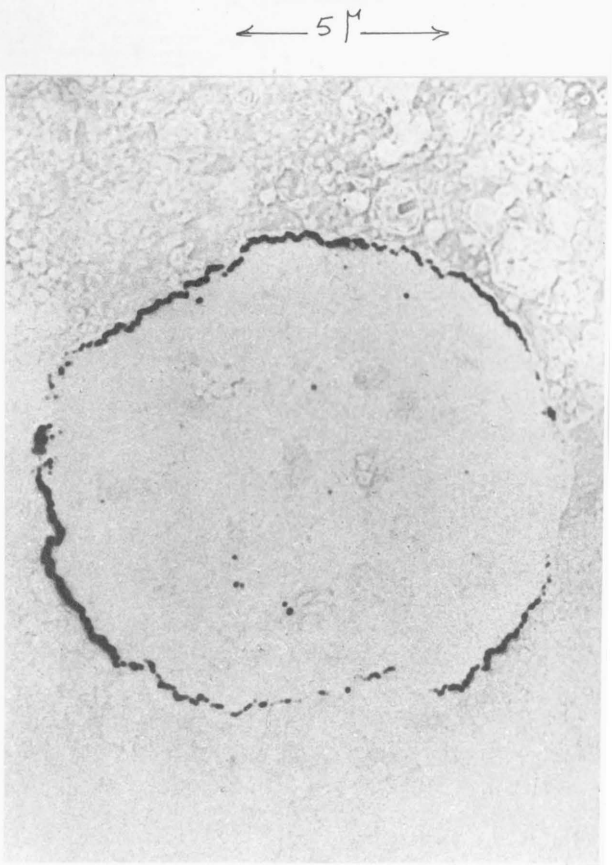


Figure (6.B) Second section of appearance of reaction spot on iron film.

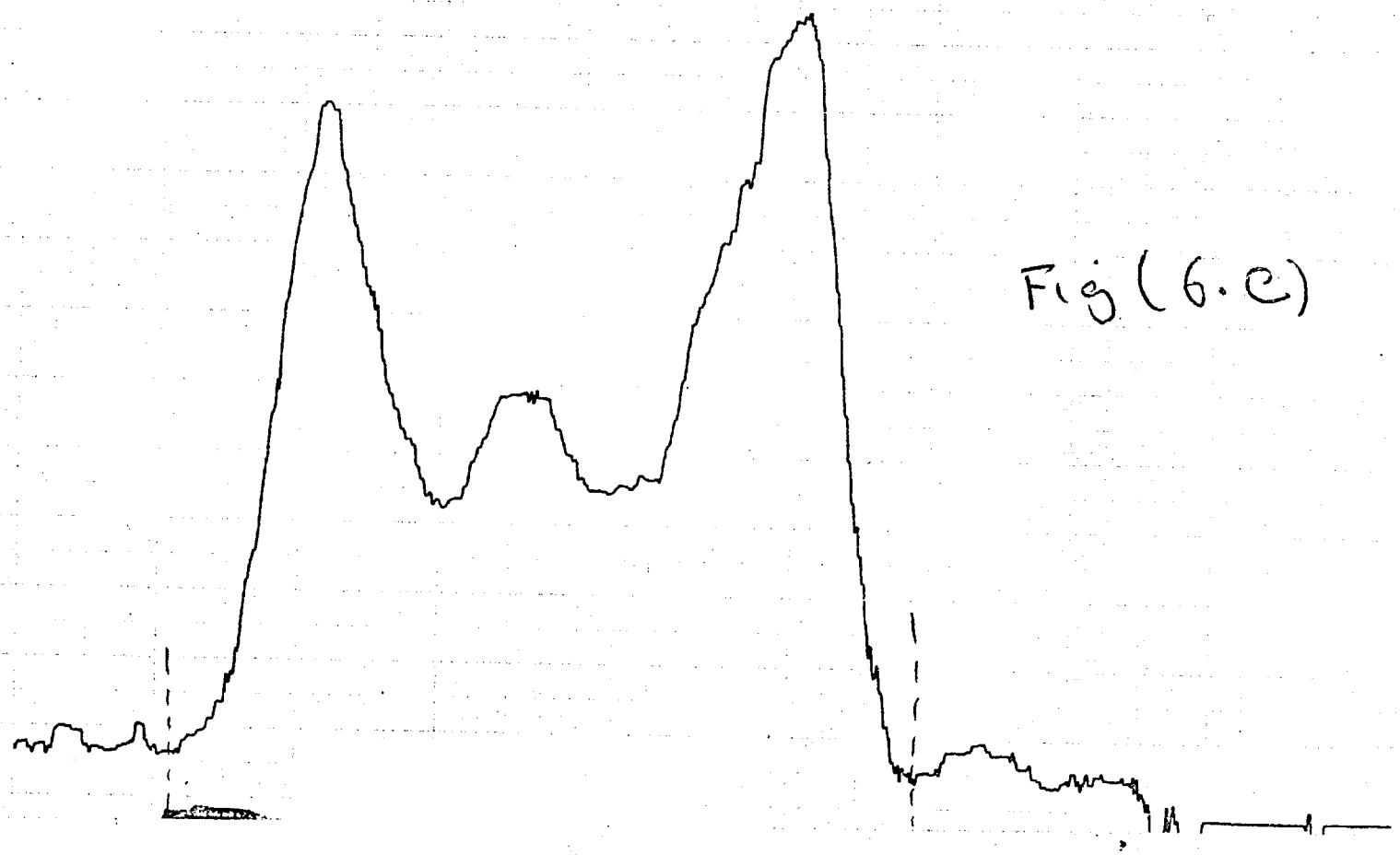


Fig (6.c)

Microdensitometry from spot with bright ring on its perimeter

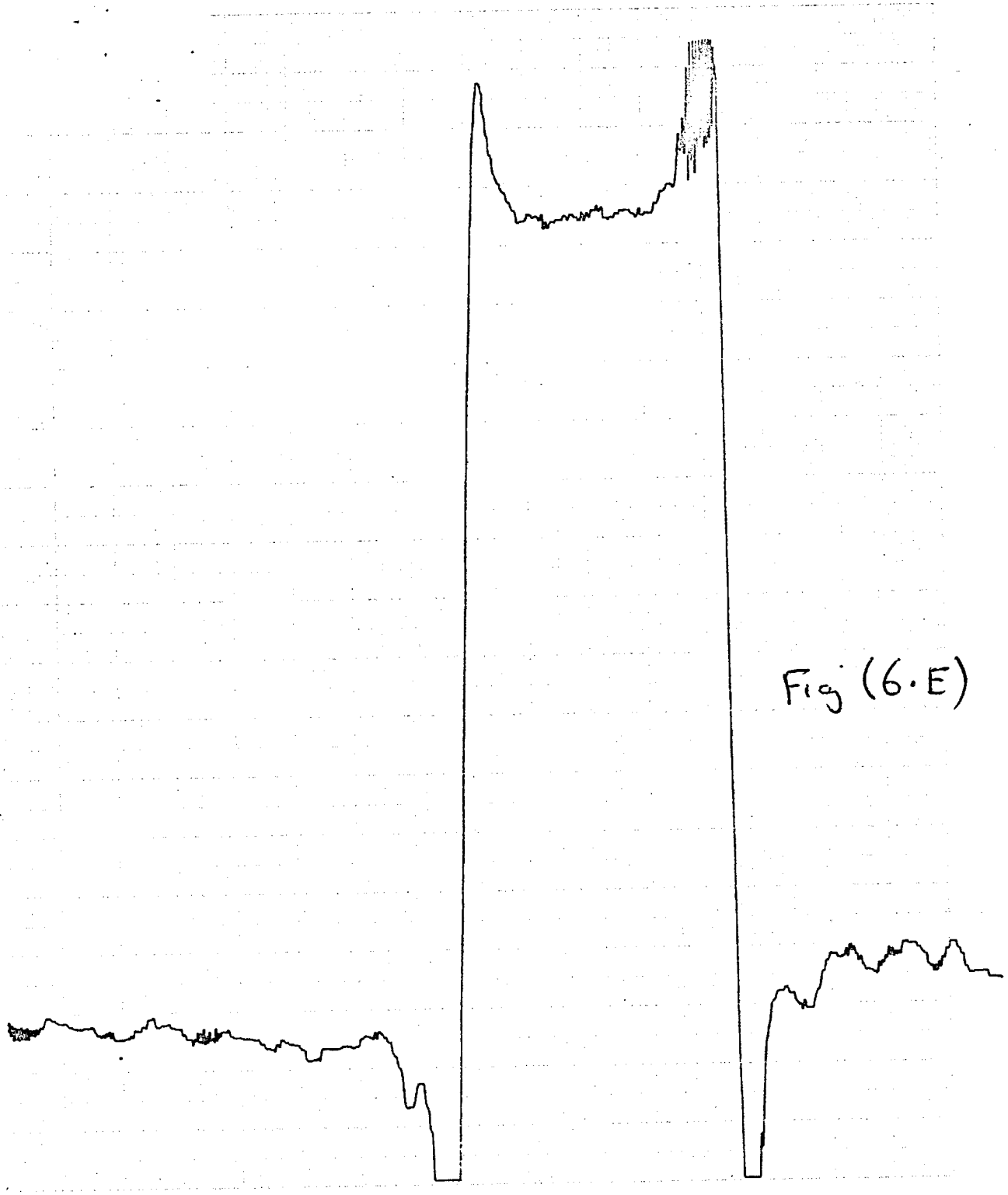


Fig (6.E)

Microdensitometry of Spot with Opaque Ring

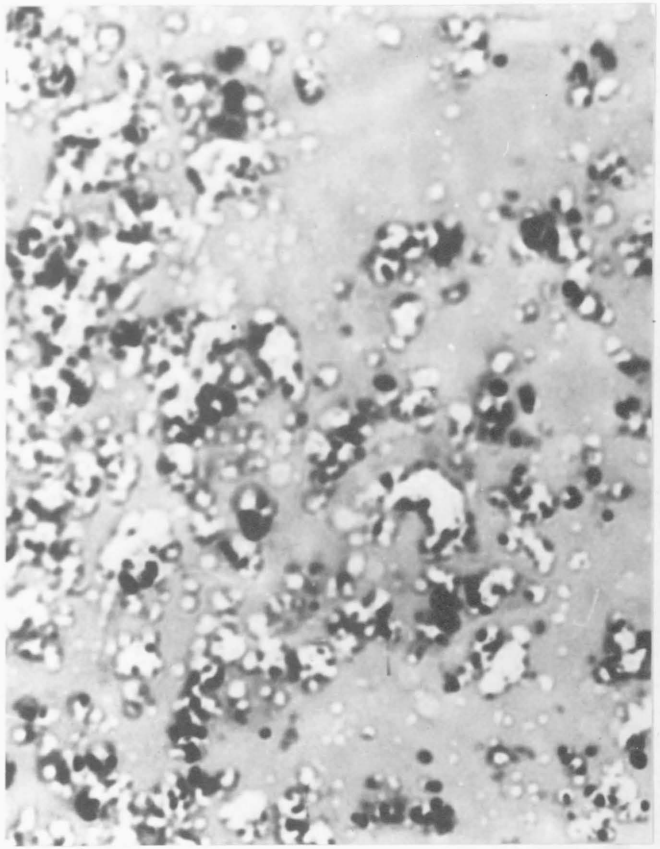


Figure (6.13) Electron micro-photograph of reaction spots contain solid on 3rd stage of compactor. (outdoor pollution).

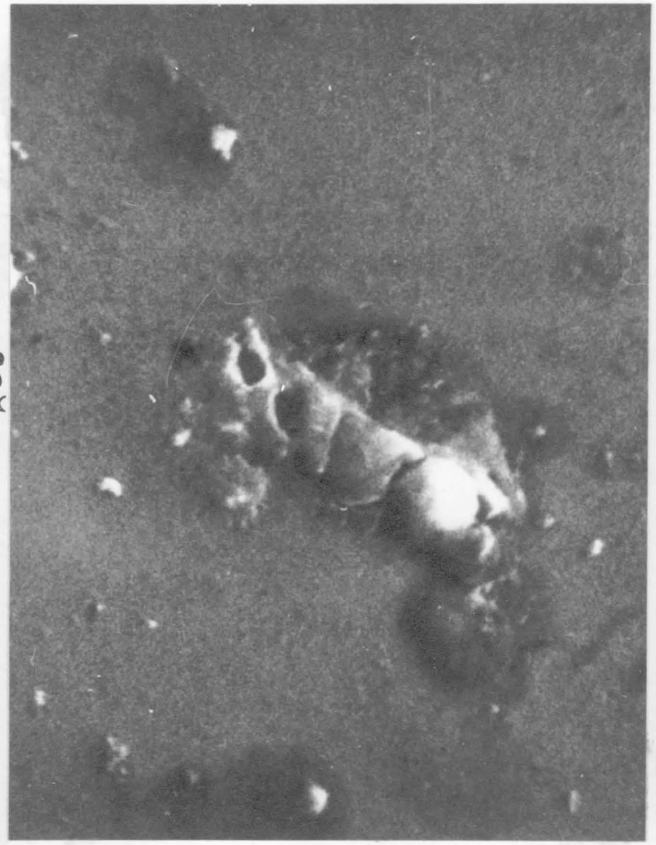


Figure (6.13) Scan electron microphotograph of a reaction spot contains solid.

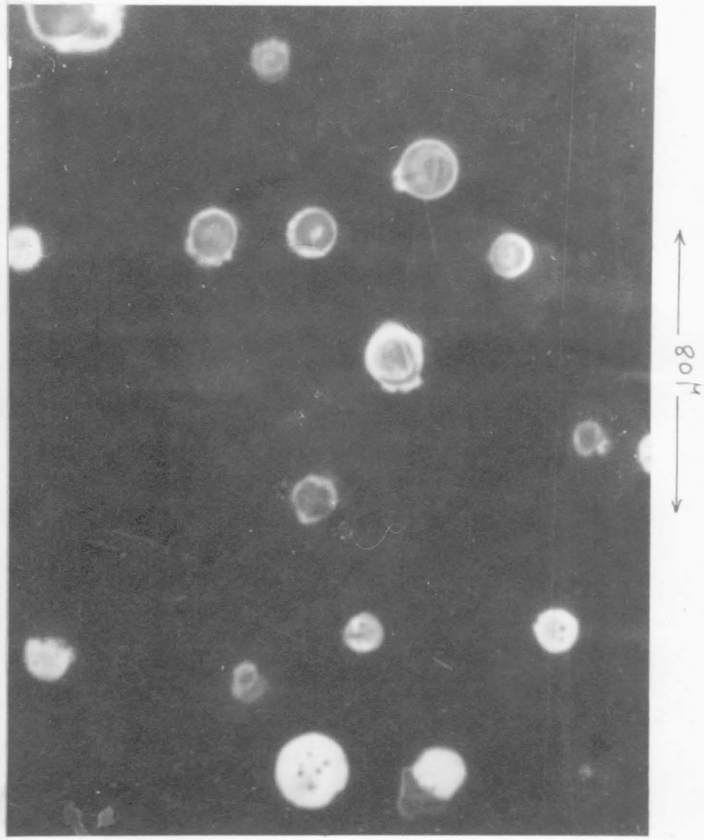


Figure (6.11) Reaction spots of 2N acid and made by nebulizer on iron film.

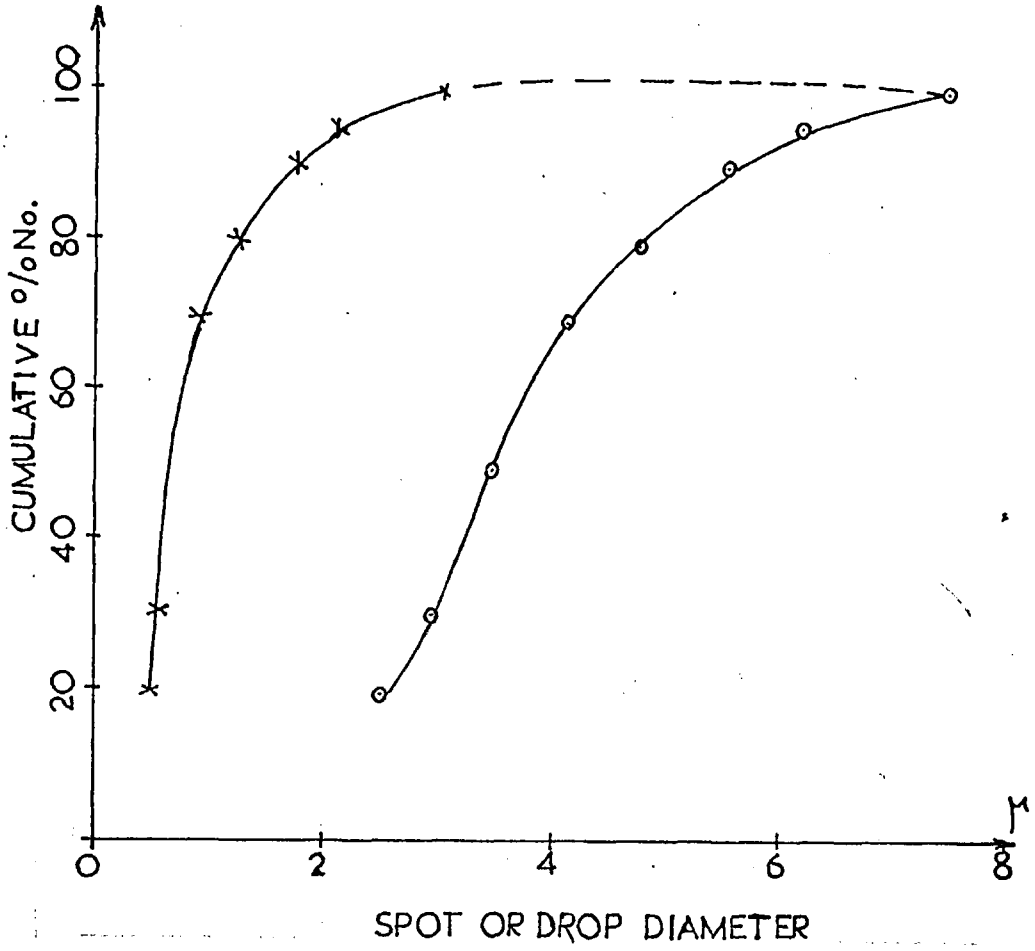


Figure (6.9) Reaction Spot of 2N acid Drop on 250 A° Nickel.

2N Acid drop in Silicone Layer

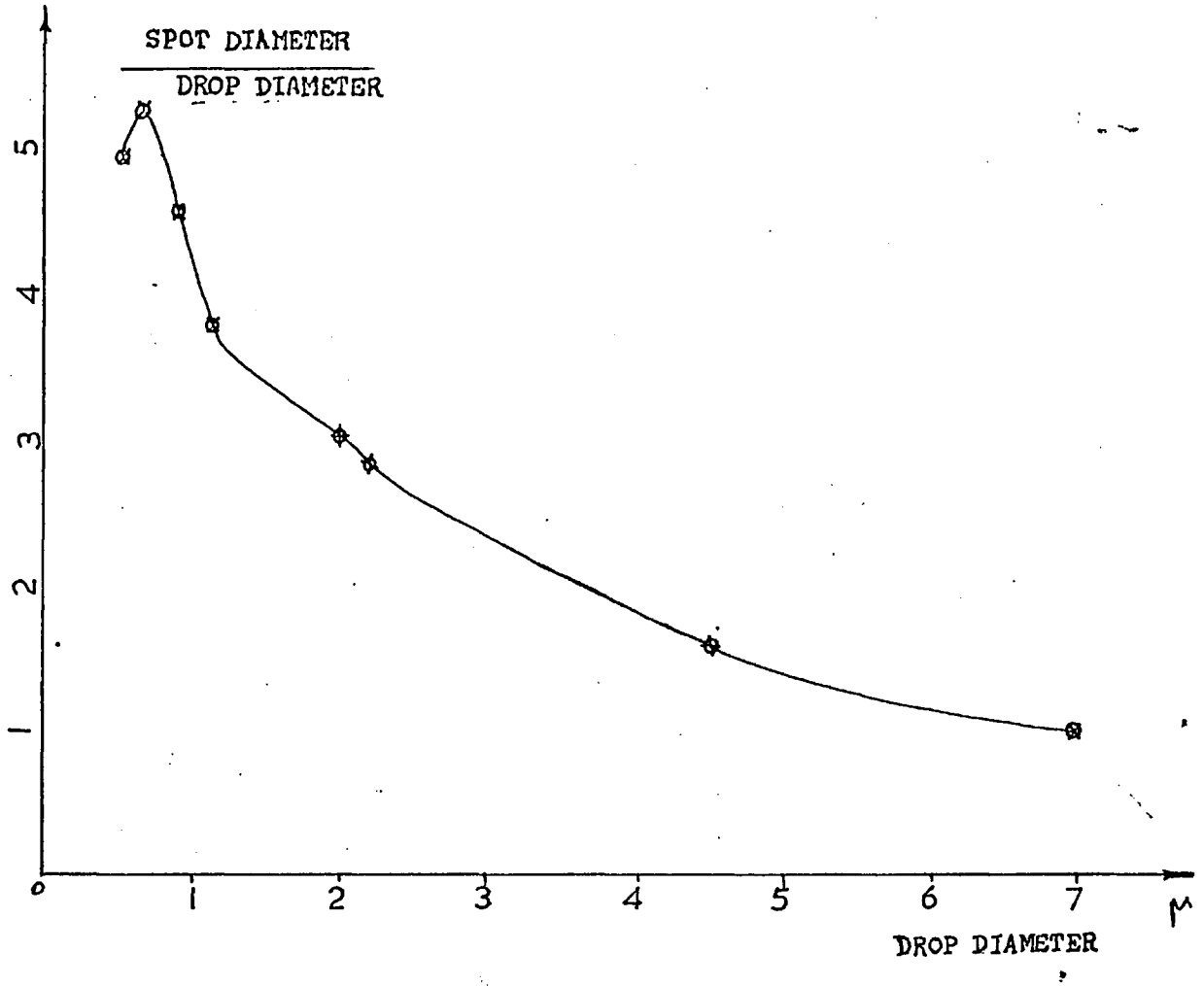


Figure (6.10) Ratio of Spot Diameter to Drop Diameter vs. Drop Diameter

The nickel film was then washed and dried. The film, and the drops collected in the silicone layer, were both studied with an optical microscope. A standard graticule was used for sizing.

A) On nickel film: Although 600 spots would be statistically sufficient for a size distribution, 3500 spots were sized from 3 slides which were exposed at the same time to the same acid mist (all coated with 250 A^{O} nickel). The reaction spots were studied using incident and transmitted light.

B) In the silicone layer: 900 droplets in suspension were sized under the same conditions as used for spot measurement. The size distributions are plotted in Figure (6.9) and the ratio of spot/drop size in Figure (6.10). The acid drop size distribution curve has a statistically sufficient number of results in the range (1 - 3)μ. Only 15 droplets were found with diameter bigger than 6 μ. No constant ratio is found between drop diameter and spot diameter since ratio shows rapid decrease when the drop size increases: Figure (6.9) and (6.10).

(6.3) Light transmission measurement through spots:

(6.3.1) Introduction: When microphotographs from nickel and iron were studied, another important point was discovered. As can be seen from Figure (6.11), spots of the same diameter do not all show equal transparency.

Thus although the reaction spots have the same diameter, the drops which caused them did not have the same acid content.

In other words, two droplets of different size (normality assumed to be the same), produce the same size reaction spots but with different depth of pits. Evidently, one dimensional sizing of spots seems to be quite misleading, and measurement of the volume of the pits appears to be the only way of determining the size or acid content of the drops.

This can be done, as described in the last chapter by light measurement through the spots.

(6.3.2) Light measurement through spots on iron film:

For spots in range of size (6-7) μ, brightness or the integral of intensity over a spot was spot was measured using the sensitive cell of an exposuremeter. Nearly 50 spots were studied (all with the same size) and the arithmetic mean of the exposure meter readings was taken as a measure of brightness or integral of intensity.

1) Condition of microscope: 12.5 x eyepiece, 63 x objective.

2) Condition of exposure meter: x10 readings are noted in all cases.

Figure (6.12) gives a plot of log exposure meter readings on spot in average against thickness of iron film for three concentrations of acid droplets.

Brightness or over all intensity of very small spots 2 μ diameter could not be measured using a photometer cell and microscope, because of irregular variations in the background itself, so that experimental error increased markedly. For this reason, optical and electron micrographs were taken and

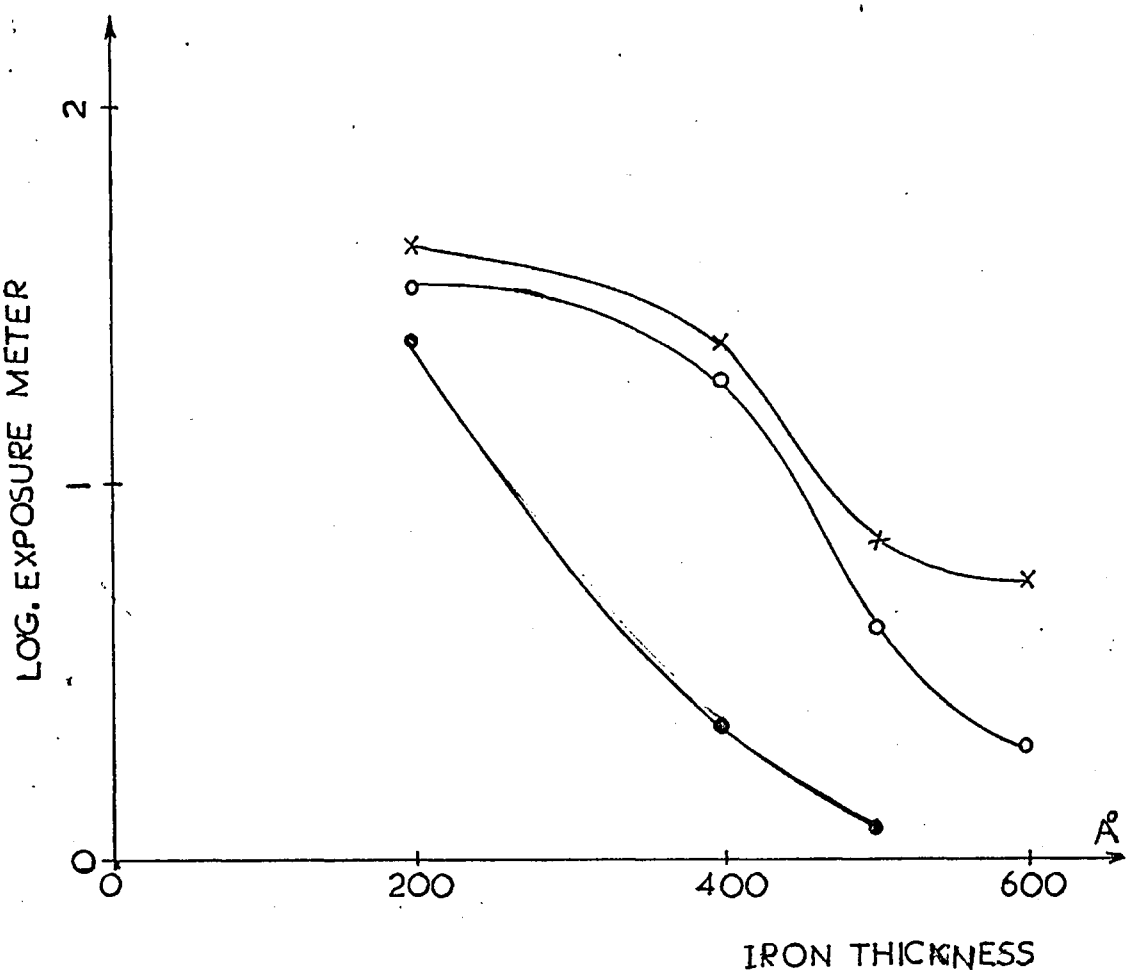


Figure (6.12) Log. Brightness of Reaction Spot of Sulphuric Acid on Iron with Different Thickness.

•—•10% Acid, o—o—o 45% and x—x—x 100%.

density of each spot was directly measured from negatives. Care was taken not to measure unusual spots with highly local attacks such as in Figure (6.8) where the average of density is meaningless.

(6.4) Studying outdoor pollution:

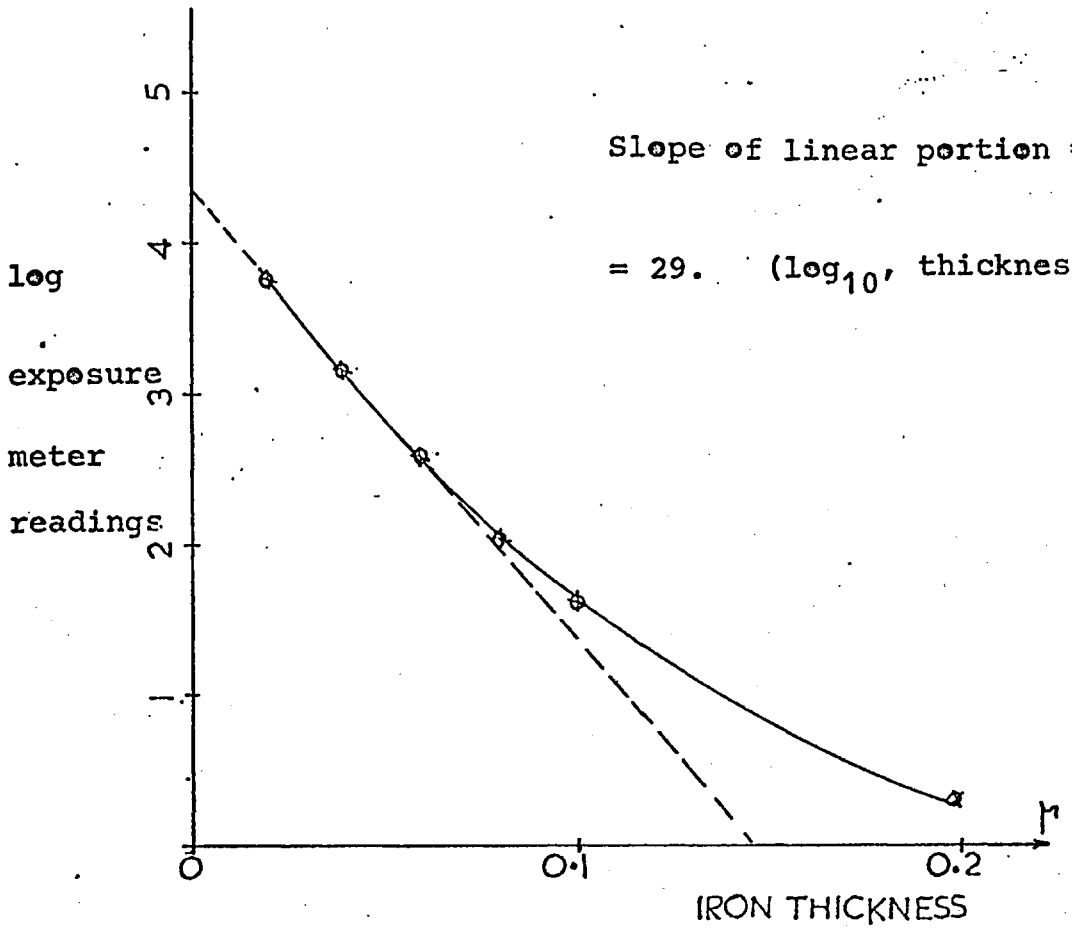
(6.4.1) Outdoor pollution is much more complex since acid droplets are associated with solid. Figure (6.13) shows one of the cases where solid particles obstruct most of the light which should be transmitted through reaction spots. In this case light transmission method fails to provide any significant estimation of size or concentration of atmospheric acid droplets.

(6.4.2) Light measurement through spots of acid drops containing solid

An attempt was made to find if there is any regular relationship between volume or mass of acid condensed on solid particles and the diameter of solid or the brightness of the spots formed. In other words, any relation between $\frac{\text{clear area}}{\text{solid area}}$ and brightness of reaction spot is sought.

A glass slide coated with 500 A^{O} iron was exposed in the third stage of a cascade impactor to outdoor pollution on 11.10.69, when the outdoor temperature was 14 ^{O}C and R.H. was 75%. About 70% of the spots found on this stage were associated with solid, mainly black particles.

Optical microscopewas used and brightness or transparency of each thickness supported on glass slide were measured by measuring brightness of 15 randomly chosen fields and arithmetically averaging



Slope of linear portion = $\frac{4.29 - 1.3.6}{0.1}$

= 29. ($\log_{10}$, thickness in)

Figure (6.14) Log. exposure meter reading (x1000) for unexposed iron film.

meter readings.

Table (6.1) shows transmission of unexposed iron film with different thicknesses. Measurement on each thickness shows that the mean error due to difference on thickness on one slide does not exceed $\pm$ 18% for thickness equal to 200 A^{o}, and decreases as the thickness increases.

1) Condition on microscope: 12.5 x eyepiece and 63 x objective.

2) Condition of exposure meter: x 1000 readings are noted or calculated for each case.

Acid droplets assumed to be 2N. The diameter of acid drop responsible for spot formation is calculated from the volume of dissolved iron in the pit formed. Results are illustrated in Figures (6.15) and (6.16). No linear or regular relationship could be found either between spot diameter and pure drop diameter or between logarithm of spot brightness and spot diameter.

(6.4.3) When outdoor pollution was collected on a metal film, the acid particles which contained solid usually made pits of irregular shape. The minority of particles without solid produced pits which were regular in shape; they were actually more regular than pits from laboratory-made acid droplets.

This is quite promising for the application of the light transmission method for atmospheric acid analysis. In microdensitometric analysis of

Thickness of iron	Log. exp. met. reading
0.02	3.72
0.04	3.09
0.06	2.46
0.08	2.00
0.10	1.67
0.20	0.30

Table (6.1) Transmission measurement through unexposed iron

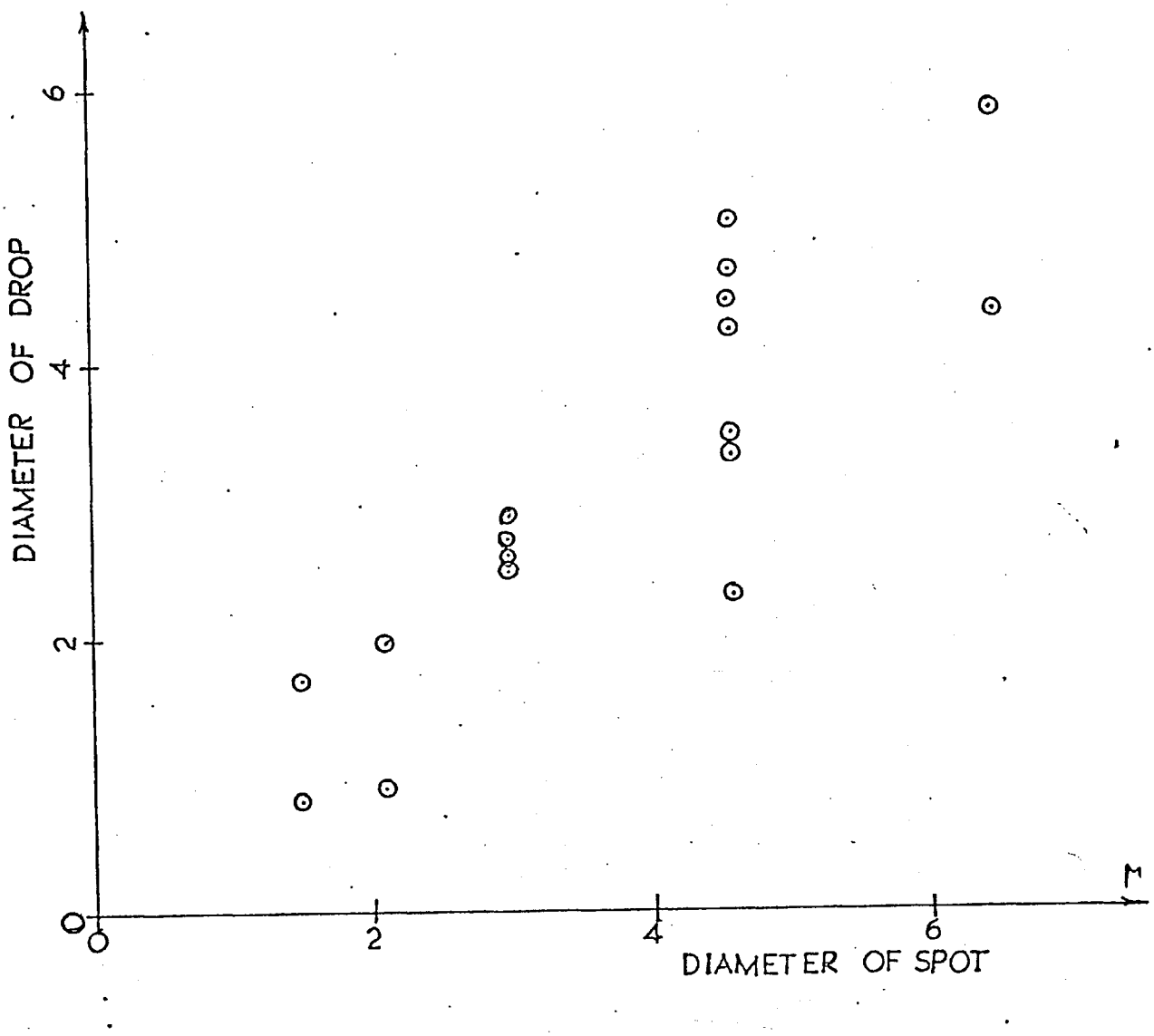


Figure (6.15) Calculated Diameter of 2N Acid Droplet vs. Diameter of Reaction Spot

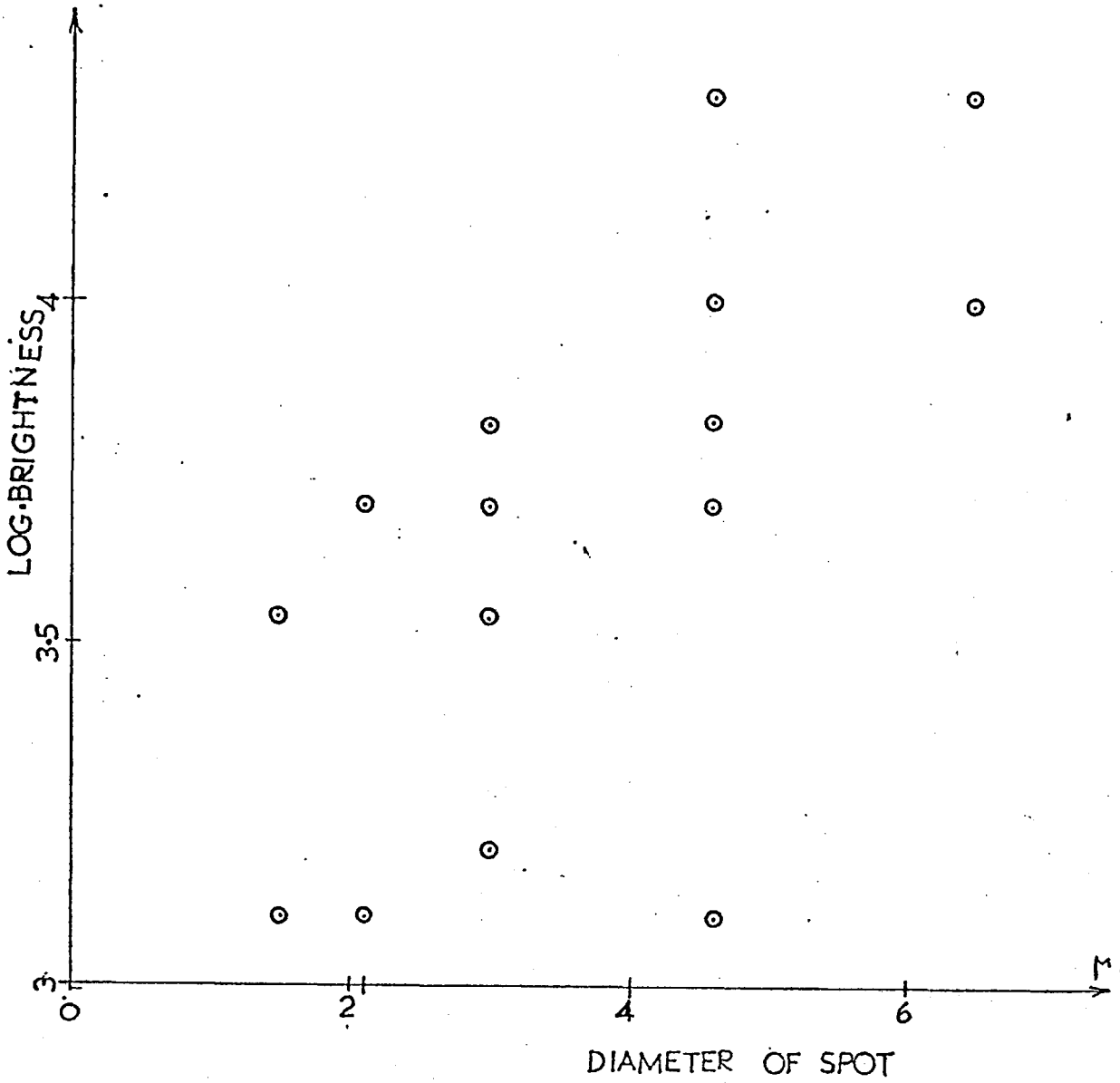


Figure (6.16) Log. Brightness of Solid Containing Spot vs. Diameter of Spot.

photographs of such pits taken through the electron microscope, the density looks quite even or in other words the pit formed must be nearly cylindrical. Figure (6.17) gives density plotted by microdensitometer across the reaction spots made by outdoor acid on 200 A° iron. Figure (6.18) shows the microphotograph of the spots which were analysed by microdensitometer.

(6.4.4) Measure of total field transmission: The theory of this part is completely explained and worked out in last chapter (Section (5.7)). This part of the investigation is done to measure total concentration of sulphuric acid in air.

Experimental conditions:

Date and time of sampling: 10.30 on 21.11.69.

Weather conditions: calm, foggy and cloudy.
Temperature was 17 $^{\circ}C$ and R.H. = 82%.

Instrument = 5-stage cascade impactor.

Stages coated by: 400 A° iron.

Duration of sampling: 10 minutes.

Experimental device: Exposed metal coated slides were washed with distilled water.

Slides were studyied: by optical microscope using light transmission, 12.5 x eyepiece and 63 x objective.

Time of study: Approximately 60 minutes after sampling.

Results: 1) on first stage, there was no bright spot at all.

2) On second stage, although a few, wide spread spots could be seen, there were not enough to be studied by this method. (50 spots on all deposition area).

3) On third stage, 960 spots counted on each

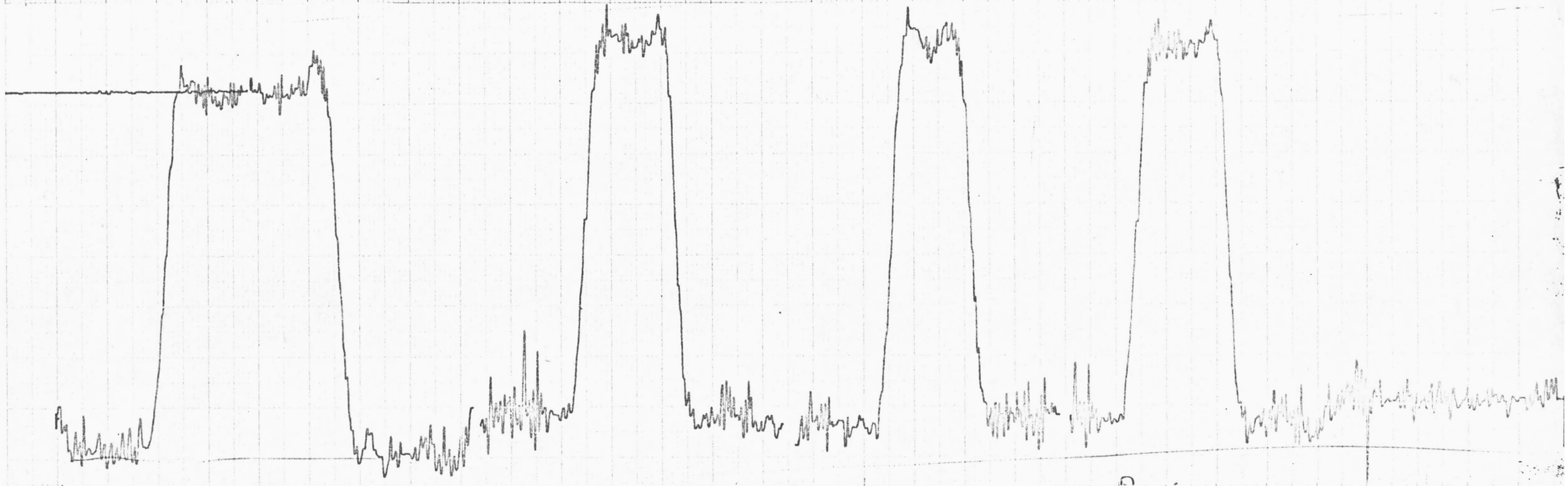


Fig (6-17)



Figure (6.4.4.2) Reaction spot of outdoor acid droplets on fourth stage of cascade impactor (on iron film).

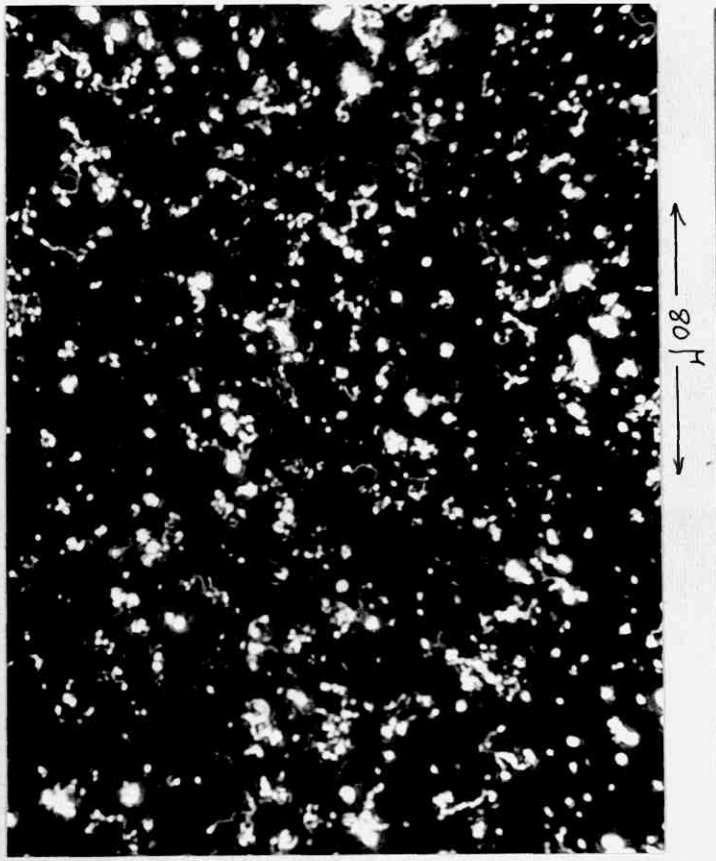


Figure (6.4.4.1) Reaction spots of outdoor acid droplets on third stage of cascade impactor (on iron film).

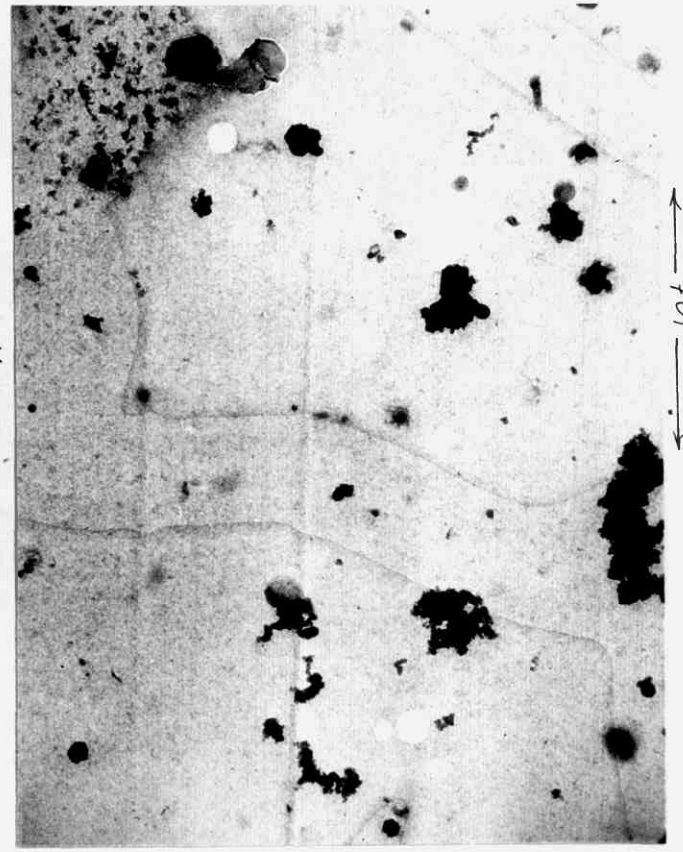


Figure (6.18) Electron microphotograph of reaction spot of outdoor acid droplets. (on nickel film).

field in average. Light transmission was measured through 10 fields, each with nearly the same number of spots. Logarithm of average (arithmetic mean) of these 10 readings then was taken on plotted chart for unexposed iron and average of thickness on deposited area was then derived. Total metal dissolved on all deposition area was calculated. Acid assumed to be 2N. So total acid content in droplets deposited on this stage was then worked out:

Total mass of dissolved iron = 3.266×10^{-6} g.

Total mass of acid responsible = 5.82×10^{-6} g.

Total air passed through stage = 262.5 litre.

Acid concentration in air = $\underline{22\ \mu g/m^3}$.

4) On fourth stage, because the number concentration of spots on different parts of the deposition area was not the same, 50 different areas were chosen in which solid particles had least effect obstructing light through spots. The results from the same calculation which is done for third stage are:

Total mass of iron dissolved = 4.65×10^{-6} g.

Total mass of acid responsible = 6.39×10^{-6} g.

Total volume of air passed = 262.5 litre.

so acid concentration = $\underline{25\ \mu g/m^3}$.

Therefore the total acid concentration for droplets in the range of (0.4 - 2) μ is approximately equal to 47 $\mu g/m^3$.

Since Waller (1963) showed that nearly 50% of total sulphuric acid is trapped on the fifth stage of the impactor on filter paper, the concentration is estimated to be 90 $\mu g/m^3$. This sampling showed the highest concentration of acid in samples taken during the period September 1968 to April 1970 (samples were taken only on days when pollution seemed to be high). Figures (6.4.4.1) and (6.4.4.2) show photograph of third and fourth stage from above sampling.

This simple and fast method for acid concentration measurement is not completely developed in this investigation, since the aim of this work was mainly to study individual droplet. However, it is clear that this method of measuring total acid might be improved by attention to the following points.

a) A more efficient method should be worked out for removing solid particles deposited, especially on the fourth stage of the impactor.

b) The metal film should be as uniform as possible in thickness all over the glass slide.

c) Care should be taken to provide even and stable illumination throughout the microscopic measurements.

The application of light transmission method for estimating total concentration of acid in air is most suitable either on days when the concentration of acid is high or in locations where the concentration is specially high for some local or industrial reasons.

(6.4.5) Light transmission measurement through individual spots:

The aim of these measurements is to provide a method for size distribution measurement of atmospheric sulphuric acid droplets. As mention in section (6.2), sizing of reaction spots did not provide any linear or constant relationship between drop diameter and reaction spot diameter. For this reason, the total energy of light transmitted through the spots is measured for individual spots and acid content in droplets can be calculated. Assuming that the R.H. is known, or in other words, that the acid concentration in drop is known, the size of the acid droplet can be accurately derived. In this investigation, only electronmicrographs are used for density measurement. This is done for these reasons: 1) Electron microscope study can cover the whole size range of spots when outdoor acid droplets are sampled (0.02 - 20)μ. [illegible] were used in [illegible]

2) Plates were more convenient than films for densitometry.

3) The illumination of the electron microscope viewing field was much more even than in the optical one.

4) Plates were calibrated for densities up to 1.5 and their response was measured and plotted in this investigation.

The specimen for electron microscopy was prepared as described in the last chapter from metal film exposed to outdoor pollution and the photograph was taken through the Siemens electron microscope.

As described in the literature survey, for electron absorption through a thin layer, the formula is:

$$I = I_c \, e^{-S_t \times \rho t}$$

where S_t is called total mass scattering cross section of electron. This factor is constant as long as the microscope condition is constant. Since I/I_o can be measured by measuring spot density, then for calculating ρt (which provides t if ρ is known), S_t should be accurately determined in advance.

Three different thickness iron films were made in the vacuum unit and measured accurately by an interferometric method which gave the average thickness on each slide with an accuracy of $\pm$ 10 A°.

Specimens were prepared from these three unexposed iron films and 10 photographs were taken from each thickness. Fog, background and specimen density were measured on each microphotograph using a microdensitometer. The fog density was subtracted on each plate from the background and specimen density and S_t was calculated for each plate:

$$I_S = I_B \, e^{-S_t x \, \rho t} \quad \text{or} \quad \frac{I_B}{I_S} = e^{S_t \times \rho t}$$

(ρ is assumed to be density of bulk iron).

$$\frac{D_B - D_F}{D_S - D_R} \propto \frac{I_B}{I_S}$$

$$\text{so} \qquad \log\left(\frac{D_B - D_F}{D_S - D_F}\right) = 0.43 \times \rho \times t \times S_t$$

By knowing D_B, D_F, D_S and t, S_t can be calculated. S_t is calculated for each thickness on 10 plates and averaged for each thickness. Then the arithmetic mean for the three different thicknesses is calculated and the average error the the mean

$$\text{average error} \simeq \pm \frac{\Sigma\,(+v)}{n\sqrt{n}}$$

$$S_t = (4.41 \pm 0.16) \times 10^4 \ \frac{cm^2}{g}$$

Since S_t is known, for the same condition of the electron microscope, the electron absorption equation can be written for spot and adjacent background as follows:

$$\log \frac{I_s}{I_B} = S_t\left[\rho\,(t_B - t_s)\right] \times \log e$$

so

$$\log \frac{D_s}{D_B} = 0.43 \times 4.41\ (\rho t)$$

where D_s, D_B are densities of spot and background respectively and $(t = t_2 - t_1)$ represents the depth of the pit.

The response of the densometer was linearly proportional to density within the calibrated range of density (0.2 - 2.0).

Thus:

$$\log\left(\frac{\text{response to spot}}{\text{response to same area of background}}\right)$$

gives ρt, i.e. the weight of metal dissolved per unit area.

$$\rho t = \frac{\log \frac{R_S}{R_B}}{0.43\ S_t}$$

By knowing the area of the spot illuminated, the total mass of dissolved metal can be calculated. This method was applied to pure spots (without solid) on iron film 200 A° thick exposed to outdoor pollution.

The outdoor R.H. at the time of sampling was such that the acid could be assumed to be 2N, and the size of the acid drop could easily be calculated. Fortunately, on the third and fourth stages of a sample taken by cascade impactor outdoors on 11.12.69., 43 spots could be found which had no sign of solid.

The density of these 43 spots was measured from negatives of their electron micrographs with a microdensitometer. Care was taken to avoid measurement of any part of the adjacent background which had any trace of solid materials. The results are tabulated in table (6.2). Because the number of spots measured was not statistically sufficient for plotting the size distribution, and they were only from 3rd and 4th stages, no size distribution curve is plotted.

Less than stated diameter μ	No.	Cum. % No.
0.45	2	4
0.55	9	26.2
0.80	15	62.0
1.00	12	90.6
1.80	3	97.7
4.00	1	100.0

Table (6.2) Calculated size of 2N atmospheric acid droplets

Proportional error = $\frac{\text{magnitude of error}}{\text{magnitude of diameter}}$

was calculated for each drop size due to estimation on each measurement which was done. The amount of error calculated to be 12.5% for diameter equal to 0.45 μ and percentage of error decreased as drop size increased.

CONCLUSION

Application of this method for size and concentration measurement of atmospheric sulphuric acid is theoretically proved to be quite reasonable for rather dilute and small acid droplets. If for any reason the acid droplets become very big or very concentrated, the method fails to provide any correct analysis for this situation. In suitable conditions, where the light transmission measurement provides an accurate measure of size and concentration of atmospheric acid drops, two types of error reduce the accuracy of the method. First, systematic errors are involved, as explained and calculated for one common situation in Chapter 5, Section (5.9). Calculations show that the error is less than 10% when the droplets are 1.5 μ in diameter, and even for 2N acid drops up to 2 μ diameter the error is still less than 15%. From the results in Table (5.9.1), it can be seen that simply by developing a method which causes better spread of droplet on metal film, this type of error could be markedly reduced. The second type of error can be called experimental error. In this investigation, this error is quite complicated because several different instruments are used, and each has a different accuracy. Simpler methods would have been better, though too expensive. For example, the latest (West German) Zeiss microscope with photometer is capable of accurate measurement of brightness on a field of diameter of 1 μ or less. If this had been available, the work could have been [illegible] the complexity of

done much more easily, and without the complexity of photography.

Also, the accuracy of the experimental work could be increased by avoiding experimental errors due to electron microphotographs analysis. Altogether, the method in principle is quite capable of estimating 10^{-15} gr acid with $\pm$ 15 % error. Any improvement in the whole technique could reduce both type of error and hence increase the accuracy and applicability of method.

In the last part of the experimental work, where size of acid droplets were calculated from brightness of reaction spots (Section (6.4.5)), it was found that in some cases the diameters of the reaction spots were very similar to those of the droplets. Experimentally the ratio of the spot diameter to drop diameter ranged from (0.8 - 2.1). But the most important point is that on the 4th stage of the impactor where the sampling velocity is bigger than on the 3rd stage, the spots were usually nearly equal in size to the calculated drop diameter.

This result does not amount to proof, but it does suggest that sampling velocity may affect the contact angle and hence the spot size.

REFERENCES

1. Adam and Livingston, Nature, Lond, 182, 128, (1958).
2. Allen, T., "Particle size measurement", (1968).
3. Allen, T., London University M.Sc. Thesis, (1962).
4. Billings., C.E. and Silverman, L., J.Air.Poll. Cont. Asso., 12, 582, (1962),
5. Burge, R.E., et al., J. Biophys. and Biochem. Cytology, 8 (1960).
6. Buckholz, F., and McPhail, M., Rev. Scient. Instrum., 31, 132, (1960).
7. Chopra, L., "Thin Film Phenomena", (1969).
8. Clegg, P.L., and Crook, A.W., J. Sci. Instrum., 29, 209, (1952).
9. Commins, B.T., Analyst, 88, 364, (1963).
10. Coulson, and McEllison, British,J.Appl.Phys., 14, 899, (1963).
11. Davies, C.N., Proc. Phys. Soc., 57, 259, (1947).
12. Dwyer, J.L., "Contamination analysis and control", (1966).
13. Einstein, Ann. Phys, LPz, 17, 549, (1907).
14. Ferguson, J.S., et al., JAPCA, 16, 669, (1966).
15. Fuchs, N.A., "Evaporation and growth of particles in gaseous media", (1959).
16. Fuchs, and Petrjanoff, Nature, 139, 111, (1936).
17. Fuchs, N.A., Z.Phys., 89, 736, (1934).
18. Goetz, A., J. Air Poll. Cont. Assoc., 12, 479, (1962).

Goyer [illegible], E., J. Phys., 42 [illegible], [illegible].

19. Goyer, G., and Handler, G., J. Met. ., 12, 569, (1955).

20. Hall, C.E., "Introduction to electron microscopy".

21. Hayashi, et.al., Bull. Nat. Inst. Indust. Health, 6, 35, (1961).

22. Heavens, O.S., Brown M.M. and Hinton, V., Vacuum, 9, 17, (1959).

23. Holland, L., "Vacuum deposition of thin films", (1956).

24. Hopkins, H.H., "Optical image assessment using frequency response technique".

25. Horstman, S.W., and Wagman J., Amer. Ind. Hyg. Asso. J., 28, 523, (1967).

26. Jacobs, M.B. et.al., Int. J. Air Wat. Poll., 6, 205, (1962).

27. Jorgenson, P.J., J. Chem. Phys, 37, 874, (1962).

28. La Mer, V.K., Inn. E.C.Y. and Wilson I.B., J. Coll. Sci., 5, 471, (1950).

29. Lee, R.E. and Wagman, Amer. Ind. Hyg. Asso. J., 22, 348, (1966).

30. Lipper, M. Ameri. Ind. Hyg. Asso. J., 22, 348, (1961).

31. Lodge, J.P. and Mavl'k, Int. J. Air Poll., 3, No. 4, 249, (1960).

32. Lodge J.P. and Ferguson J.S., Analysis Chem., 32, 1206, (1960).

33. Lowless, K.L., J. Vacuum Sci. Tech, 2, 24, (1965).

34. Mason, B.J., and Jayaratne, O.W., J.Sci. Instrum., 40, 247, (1963).

35. Martin, L.E., "Optical Measuring Instrument".

36. Mercer, T.T., Amer. Ind. Hyg. Asso. J, 26, 236, (1965).

37. Mellor, E.W.,"Higher mathematics".

38. Myers, L.M., "Electron optics",

39. Orr, C., et.al., J. Colloid Sci., 13, 472, (1958).

40. Osmond, F., "The microscope analysis of metals" (1962).

41. Palatnik, L.S., Boiko, B.T., and Fuks, M.J., (1966).

42. Prewette, W., and Walton, V., Brit. J. Appl. Phys., 9, 78, (1958).

43. Rapaport, E., and Weinstoke, S.E., Experientia, 11, 363, (1955).

44. Rolinson, T.S., Proc. Phys. Soc. London, B65, 910, (1952).

45. Rol, P.K., D.O., and Kistemaker, J., Proc., 3D, Intern. Congr.Vacuum Tech., Stuttgart, 1, 75, (1959).

46. Rose, H.E., J.Appl.Chem., 2, 80, (1952).

47. Ryley, D.J. and Wood, M.R., J.Sci.Instrum., 40, 303, (1963).

48. Sears, F.W., "Principles of Physics".

49. Schechter, R.S., AICHE Journal, 15, (1969).

50. Sinclair, D., and La Mer, V.K., Chem. Revs., 44, 245, (1949).

51. Smoluchowsky, M., Von.Z.Phys.Chem., 92, 129, (1917).

52. Stein, F., J. Powder Technology, 2, No. 6, 327, Sep. (1969).

53. Stairmand, C.J., Proc. Roy. Soc., A., 307, (1968).

54. Takahashi and Kazato, K., J.Appl.Phys., 20, 993, (1949).

55. Vasicek, A., "Optics of thin films".

56. Waller, R.E., et.al., Int. J.Air Wat.Poll., 7,779, (1963).

57. Waller, R.E., Int.J.Air Wat.Poll.,7,773,(1963).

58. Witby et.al., J.Air Wat. Poll., 9, 263, (1965).

59. Wilson, M.J.G., Proc.Roy.Soc.A, 300, 215, (1968).

60. Wood, E.A., "Crystals and light",